PHYSICAL REVIEW D **88,** 114008 (2013)

Coupled-channel analysis of the possible $D^{(*)}D^{(*)}$, $\bar{B}^{(*)}\bar{B}^{(*)}$ and $D^{(*)}\bar{B}^{(*)}$ molecular states

Ning Li,[1,2,*] Zhi-Feng Sun,[3,4,†] Xiang Liu,[3,4,‡] and Shi-Lin Zhu[1,5,6,§]

[1]*Department of Physics and State Key Laboratory of Nuclear Physics and Technology, Peking University, Beijing 100871, China*
[2]*Institut für Kernphysik and Jülich Center for Hadron Physics, Forschungszentrum Jülich, D-52425 Jülich, Germany*
[3]*School of Physical Science and Technology, Lanzhou University, Lanzhou 730000, China*
[4]*Research Center for Hadron and CSR Physics, Lanzhou University and Institute of Modern Physics of CAS, Lanzhou 730000, China*
[5]*Center of High Energy Physics, Peking University, Beijing 100871, China*
[6]*Collaborative Innovation Center of Quantum Matter, Beijing 100871, China*

(Received 22 November 2012; revised manuscript received 17 September 2013; published 3 December 2013)

We perform a coupled-channel study of the possible deuteron-like molecules with two heavy flavor quarks, including the systems of $D^{(*)}D^{(*)}$ with double charm, $\bar{B}^{(*)}\bar{B}^{(*)}$ with double bottom, and $D^{(*)}\bar{B}^{(*)}$ with both charm and bottom, within the one-boson-exchange potential model. In our study, we take into account the S-D mixing which plays an important role in the formation of the loosely bound deuteron, and particularly, the coupled-channel effect in the flavor space. According to our results, the state $D^{(*)}D^{(*)}[I(J^P) = 0(1^+)]$ with double charm, the states $\bar{B}^{(*)}\bar{B}^{(*)}[I(J^P) = 0(1^+), 1(1^+)]$, $(\bar{B}^{(*)}\bar{B}^{(*)})_s[J^P = 1^+, 2^+]$ and $(\bar{B}^{(*)}\bar{B}^{(*)})_{ss}[J^P = 1^+, 2^+]$ with double bottom, and the states $D^{(*)}\bar{B}^{(*)}[I(J^P) = 0(1^+), 0(2^+)]$ with both charm and bottom might be good molecule candidates. However, the states $D^{(*)}D^{(*)}[I(J^P) = 0(2^+), 1(0^+), 1(1^+), 1(2^+)]$, $(D^{(*)}D^{(*)})_s[J^P = 0^+, 2^+]$ and $(D^{(*)}D^{(*)})_{ss}[J^P = 0^+, 1^+, 2^+]$ with double charm and the state $D^{(*)}\bar{B}^{(*)}[I(J^P) = 1(1^+)]$ with both charm and bottom are not supported to be molecules.

DOI: 10.1103/PhysRevD.88.114008 PACS numbers: 14.40.Rt, 12.39.Hg, 12.39.Pn, 14.40.Lb

I. INTRODUCTION

More and more experimental observations have stimulated the extensive discussions of exotic states. The molecular state explanation to the reported charmonium-like states X, Y, Z becomes popular due to the fact that many charmonium-like states near the threshold of charmed meson pair, i.e.,

$$X(3872) \sim m_{D\bar{D}^*}, \qquad Y(3930) \sim m_{D^*\bar{D}^*}$$
$$Y(4140) \sim m_{D_s^*\bar{D}_s^*}, \qquad Y(4274) \sim m_{D_{s0}(2317)\bar{D}_s}.$$

In the past decade there is abundant literature with the study of the heavy flavor molecular states [1–23].

The concept of molecular state with hidden charm was first proposed by Voloshin and Okun thirty years ago and they studied the interaction between the charmed and anticharmed mesons [24]. Later, De Rujula, Georgi, and Glashow suggested that the observed $\psi(4040)$ is a $D^*\bar{D}^*$ molecule [25]. By the quark-pion interaction model, Törnqvist investigated the possible deuteron-like two meson bound states with $B\bar{B}^*$ or $B^*\bar{B}^*$ component [26,27]. At present, carrying out the phenomenological study of the heavy flavor molecular state is still a hot research topic of hadron physics.

*leening@pku.edu.cn
†sunzhif09@lzu.edu.cn
‡xiangliu@lzu.edu.cn
§zhusl@pku.edu.cn

Usually, the hadron configurations mainly include

$$\text{hadron}\begin{cases}\text{meson:} & q\bar{q},\quad Q\bar{q},\quad Q\bar{Q}\\ \text{baryon:} & qqq,\quad Qqq,\quad QQq,\quad \ldots\\ \text{exotic state:} & \begin{cases}\text{molecular state}\\ \text{hybrid}\\ \text{glueball}\\ \ldots,\end{cases}\end{cases}$$

where q and Q denote the light (u, d, s) and heavy (c, b) quarks, respectively. Among the conventional baryon states, the baryons with double charm or double bottom are of the QQq configuration. The SELEX collaboration reported the first observation of a doubly charmed baryon Ξ_{cc}^+ in its charged decay mode $\Xi_{cc}^+ \to \Lambda_c^+ K^- \pi^+$ [28] and confirmed it in the decay mode $\Xi_{cc}^+ \to pD^+K^-$ [29]. However, later the *BABAR* collaboration searched for Ξ_{cc}^+ in the final states $\Lambda_c^+ K^- \pi^+$ and $\Xi_c^0\pi^+$, and Ξ_{cc}^{++} in the final states $\Lambda_c^+ K^- \pi^+\pi^-$ and $\Xi_c^0\pi^+\pi^+$, and found no evidence for the production of the doubly charmed baryons [30]. The Belle collaboration reported no evidence for the doubly charmed baryons in the final state $\Lambda_c^+ K^- \pi^+$ either [31]. Although these doubly charmed baryons were not confirmed by *BABAR* and BELLE, it is still an interesting research topic to search for such doubly charmed baryons experimentally.

Besides the doubly heavy flavor baryons, it is also very interesting to study other systems with two heavy flavor quarks. The heavy flavor molecular state with two charm quarks provides another approach to investigate the hadron

states with double charm. For this kind of hadron, its typical configuration is $[c\bar{q}][c\bar{q}]$. To answer whether there exist such heavy flavor molecular states with double charm or not, in this paper we apply the one-boson-exchange (OBE) model to perform a dynamic calculation of their mass spectroscopy. This study is not only a natural extension of the previous work of the heavy flavor molecular state with hidden charm, but also provides new insight into exploring the hadron states with double charm. Besides the hadron states with double charm, we also investigate the hadron states with double bottom and the hadron states with both charm and bottom.

This paper is organized as follows. After the Introduction, we present the derivation of the effective potential in Sec. II. We summarize our numerical results and perform some analysis in Sec. III and draw some conclusions in Sec. IV. We also give some useful formulas in the Appendix.

II. FORMALISM

A. The Lagrangians and the coupling constants

In the present paper, we investigate the possible molecules of $(D^{(*)}D^{(*)})$ with double charm, $(\bar{B}^{(*)}\bar{B}^{(*)})$ with double bottom and $(D^{(*)}\bar{B}^{(*)})$ with both charm and bottom. In our study, we take into account the S-D mixing which plays an important role in the formation of the loosely bound deuteron and, particularly, the coupled-channel effects in the flavor space. We study the systems with total angular momentum $J \leq 2$. We list the channels for different systems in Tables I and II.

The Lagrangians under the heavy quark symmetry and the SU(3)-flavor symmetry read [32–35]

$$\mathcal{L}_{HH\mathcal{M}} = ig\,\mathrm{Tr}[H_b^{(Q)}\gamma_\mu\gamma_5 A^\mu_{ba}\bar{H}_a^{(Q)}], \tag{1}$$

$$\mathcal{L}_{HHV} = i\beta\,\mathrm{Tr}[H_b^{(Q)}v_\mu(V^\mu_{ba}-\rho^\mu_{ba})\bar{H}_a^{(Q)}] + i\lambda\,\mathrm{Tr}[H_b^{(Q)}\sigma_{\mu\nu}F^{\mu\nu}(\rho)_{ba}\bar{H}_a^{(Q)}], \tag{2}$$

$$\mathcal{L}_{HH\sigma} = g_s\,\mathrm{Tr}[H_a^{(Q)}\sigma\bar{H}_a^{(Q)}], \tag{3}$$

where $H^{(Q)}$ and $\bar{H}^{(Q)}$ are defined as

$$H_a^{(Q)} = \frac{1+\not{v}}{2}[P_a^{*\mu}\gamma_\mu - P_a\gamma_5] \tag{4}$$

and

$$\bar{H}_a^{(Q)} \equiv \gamma_0 H^{(Q)\dagger}\gamma_0 = [P_a^{*\dagger\mu}\gamma_\mu + P_a^\dagger\gamma_5]\frac{1+\not{v}}{2} \tag{5}$$

with $P_a^* = (D^{*0}, D^{*+}, D_s^{*+})$ or $(B^{*-}, \bar{B}^{*0}, \bar{B}_s^{*0})$ being the charmed or antibottomed vector mesons and $P = (D^0, D^+, D_s^+)$ or $(B^-, \bar{B}^0, \bar{B}_s^0)$ being the charmed or antibottomed pseudoscalar mesons. The trace acts on the gamma matrices. The axial-current A^μ is defined as $A^\mu \equiv \frac{1}{2}(\xi^\dagger\partial^\mu\xi - \xi\partial^\mu\xi^\dagger) = \frac{i}{f_\pi}\partial^\mu\mathcal{M} + \cdots$, where $\xi \equiv e^{\frac{i\mathcal{M}}{f_\pi}}$ with $\mathcal{M}$ being the exchanged pseudoscalar meson matrix given in Eq. (6). The vector current V^μ is defined as $V^\mu \equiv \frac{1}{2}(\xi^\dagger\partial^\mu\xi + \xi\partial^\mu\xi^\dagger)$. In the heavy quark limit, the heavy meson velocity is adopted as $v^\mu = (1,0,0,0)$. $F_{\mu\nu}(\rho) \equiv \partial_\mu\rho_\nu - \partial_\nu\rho_\mu - [\rho_\mu, \rho_\nu]$, where $\rho_\mu = \frac{ig_v}{\sqrt{2}}\hat{\rho}_\mu$ with $\hat{\rho}$ being the exchanged vector meson matrix given in Eq. (7). Expanding the Lagrangians given in Eqs. (1)–(3), we list the specific expressions in Eqs. (8)–(14).

$$\mathcal{M} = \begin{pmatrix} \frac{1}{\sqrt{2}}\pi^0 + \frac{\eta}{\sqrt{6}} & \pi^+ & K^+ \\ \pi^- & -\frac{1}{\sqrt{2}}\pi^0 + \frac{\eta}{\sqrt{6}} & K^0 \\ K^- & \bar{K}^0 & -\frac{2}{\sqrt{6}}\eta \end{pmatrix}, \tag{6}$$

TABLE I. The different channels for the $D^{(*)}D^{(*)}$ systems, and similarly, for the $\bar{B}^{(*)}\bar{B}^{(*)}$. S is the strangeness while I stands for the isospin of the systems. "$***$" means the corresponding state does not exist due to the symmetry. For simplicity, we adopt the shorthand notations, $[DD^*]_- \equiv \frac{1}{\sqrt{2}}(DD^* - D^*D)$ and $[DD^*]_+ \equiv \frac{1}{\sqrt{2}}(DD^* + D^*D)$.

		Channels						
S	$I(J^P)$	1	2	3	4	5	6	7
0	$0(0^+)$				$***$			
	$0(1^+)$	$[DD^*]_-(^3S_1)$	$[DD^*]_-(^3D_1)$	$D^*D^*(^3S_1)$	$D^*D^*(^3D_1)$	$\cdots$	$\cdots$	$\cdots$
	$0(2^+)$	$[DD^*]_-(^3D_2)$	$D^*D^*(^3D_2)$	$\cdots$	$\cdots$	$\cdots$	$\cdots$	$\cdots$
	$1(0^+)$	$DD(^1S_0)$	$D^*D^*(^1S_0)$	$D^*D^*(^5D_0)$	$\cdots$	$\cdots$	$\cdots$	$\cdots$
	$1(1^+)$	$[DD^*]_+(^3S_1)$	$[DD^*]_+(^3D_1)$	$D^*D^*(^5D_1)$	$\cdots$	$\cdots$	$\cdots$	$\cdots$
	$1(2^+)$	$D^*D^*(^5S_2)$	$D^*D^*(^1D_2)$	$D^*D^*(^5D_2)$	$\cdots$	$\cdots$	$\cdots$	$\cdots$
1	$\frac{1}{2}(0^+)$	$DD_s(^1S_0)$	$D^*D_s^*(^1S_0)$	$D^*D_s^*(^5D_0)$	$\cdots$	$\cdots$	$\cdots$	$\cdots$
	$\frac{1}{2}(1^+)$	$DD_s^*(^3S_1)$	$DD_s^*(^3D_1)$	$D^*D_s(^3S_1)$	$D^*D_s(^3D_1)$	$D^*D_s^*(^3S_1)$	$D^*D_s^*(^3D_1)$	$D^*D_s^*(^5D_1)$
	$\frac{1}{2}(2^+)$	$D^*D_s^*(^5S_2)$	$D^*D_s^*(^1D_2)$	$D^*D_s^*(^5D_2)$	$\cdots$	$\cdots$	$\cdots$	$\cdots$
	$0(0^+)$	$D_sD_s(^1S_0)$	$D_s^*D_s^*(^1S_0)$	$D_s^*D_s^*(^5D_0)$	$\cdots$	$\cdots$	$\cdots$	$\cdots$
	$0(1^+)$	$[D_sD_s^*]_+(^3S_1)$	$[D_sD_s^*]_+(^3D_1)$	$D_s^*D_s^*(^5D_1)$	$\cdots$	$\cdots$	$\cdots$	$\cdots$
	$0(2^+)$	$D_s^*D_s^*(^5S_2)$	$D_s^*D_s^*(^1D_2)$	$D_s^*D_s^*(^5D_2)$	$\cdots$	$\cdots$	$\cdots$	$\cdots$

TABLE II. The different channels for the $D^{(*)}\bar{B}^{(*)}$ systems. "S" is the strangeness of the corresponding system while "I" stands for the isospin of the state.

		Channels									
S	$I(J^P)$	1	2	3	4	5	6	7	8	9	10
0	$0(0^+)$	$D\bar{B}(^1S_0)$	$D^*\bar{B}^*(^1S_0)$	$D^*\bar{B}^*(^5D_0)$	$\cdots$	$\cdots$	$\cdots$	$\cdots$	$\cdots$	$\cdots$	$\cdots$
	$0(1^+)$	$D\bar{B}^*(^3S_1)$	$D\bar{B}^*(^3D_1)$	$D^*\bar{B}(^3S_1)$	$D^*\bar{B}(^3D_1)$	$D^*\bar{B}^*(^3S_1)$	$D^*\bar{B}^*(^3D_1)$	$D^*\bar{B}^*(^5D_1)$	$\cdots$	$\cdots$	$\cdots$
	$0(2^+)$	$D^*\bar{B}^*(^5S_2)$	$D^*\bar{B}^*(^1D_2)$	$D^*\bar{B}^*(^5D_2)$	$\cdots$	$\cdots$	$\cdots$	$\cdots$	$\cdots$	$\cdots$	$\cdots$
	$1(0^+)$	$D\bar{B}(^1S_0)$	$D^*\bar{B}^*(^1S_0)$	$D^*\bar{B}^*(^5D_0)$	$\cdots$	$\cdots$	$\cdots$	$\cdots$	$\cdots$	$\cdots$	$\cdots$
	$1(1^+)$	$D\bar{B}^*(^3S_1)$	$D\bar{B}^*(^3D_1)$	$D^*\bar{B}(^3S_1)$	$D^*\bar{B}(^3D_1)$	$D^*\bar{B}^*(^3S_1)$	$D^*\bar{B}^*(^3D_1)$	$D^*\bar{B}^*(^5D_1)$	$\cdots$	$\cdots$	$\cdots$
	$1(2^+)$	$D^*\bar{B}^*(^5S_2)$	$D^*\bar{B}^*(^1D_2)$	$D^*\bar{B}^*(^5D_2)$	$\cdots$	$\cdots$	$\cdots$	$\cdots$	$\cdots$	$\cdots$	$\cdots$
1	$\frac{1}{2}(0^+)$	$D\bar{B}_s(^1S_0)$	$D_s\bar{B}(^1S_0)$	$D^*\bar{B}_s^*(^1S_0)$	$D_s^*\bar{B}^*(^1S_0)$	$D^*\bar{B}_s^*(^5D_0)$	$D_s^*\bar{B}^*(^5D_0)$	$\cdots$	$\cdots$	$\cdots$	$\cdots$
	$\frac{1}{2}(1^+)$	$D_s\bar{B}^*(^3S_1)$	$D\bar{B}_s^*(^3S_1)$	$D_s^*\bar{B}(^3S_1)$	$D^*\bar{B}_s(^3S_1)$	$D_s^*\bar{B}^*(^3S_1)$	$D^*\bar{B}_s^*(^3S_1)$	$D_s\bar{B}^*(^3D_1)$	$D\bar{B}_s^*(^3D_1)$	$D_s^*\bar{B}(^3D_1)$	$D^*\bar{B}_s(^3D_1)$
	$\frac{1}{2}(2^+)$	$D_s^*\bar{B}^*(^5S_2)$	$D^*\bar{B}_s^*(^5S_2)$	$D_s^*\bar{B}^*(^1D_2)$	$D^*\bar{B}_s^*(^1D_2)$	$D_s^*\bar{B}^*(^5D_2)$	$D^*\bar{B}_s^*(^5D_2)$	$\cdots$	$\cdots$	$\cdots$	$\cdots$
2	$0(0^+)$	$D_s\bar{B}_s(^1S_0)$	$D_s^*\bar{B}_s^*(^1S_0)$	$D_s^*\bar{B}_s^*(^5D_0)$	$\cdots$	$\cdots$	$\cdots$	$\cdots$	$\cdots$	$\cdots$	$\cdots$
	$0(1^+)$	$D_s\bar{B}_s^*(^3S_1)$	$D_s\bar{B}_s^*(^3D_1)$	$D_s^*\bar{B}_s(^3S_1)$	$D_s^*\bar{B}_s(^3D_1)$	$D_s^*\bar{B}_s^*(^3S_1)$	$D_s^*\bar{B}_s^*(^3D_1)$	$D_s^*\bar{B}_s^*(^5D_1)$	$\cdots$	$\cdots$	$\cdots$
	$0(2^+)$	$D_s^*\bar{B}_s^*(^5S_2)$	$D_s^*\bar{B}_s^*(^1D_2)$	$D_s^*\bar{B}_s^*(^5D_2)$	$\cdots$	$\cdots$	$\cdots$	$\cdots$	$\cdots$	$\cdots$	$\cdots$

$$\hat{\rho}^\mu = \begin{pmatrix} \frac{\rho^0}{\sqrt{2}} + \frac{\omega}{\sqrt{2}} & \rho^+ & K^{*+} \\ \rho^- & -\frac{\rho^0}{\sqrt{2}} + \frac{\omega}{\sqrt{2}} & K^{*0} \\ K^{*-} & \bar{K}^{*0} & \phi \end{pmatrix}^\mu, \tag{7}$$

$$\mathcal{L}_{P^*P^*\mathcal{M}} = -i\frac{2g}{f_\pi}\varepsilon_{\alpha\mu\nu\lambda}v^\alpha P_b^{*\mu}P_a^{*\lambda\dagger}\partial^\nu M_{ba}, \tag{8}$$

$$\mathcal{L}_{P^*P\mathcal{M}} = -\frac{2g}{f_\pi}(P_bP_{a\lambda}^{*\dagger} + P_{b\lambda}^*P_a^\dagger)\partial^\lambda M_{ba}, \tag{9}$$

$$\mathcal{L}_{PPV} = -\sqrt{2}\beta g_V P_b P_a^\dagger v\cdot\hat{\rho}_{ba}, \tag{10}$$

$$\mathcal{L}_{P^*PV} = -2\sqrt{2}\lambda g_V v^\lambda\varepsilon_{\lambda\mu\alpha\beta}(P_bP_a^{*\mu\dagger} + P_b^{*\mu}P_a^\dagger)(\partial^\alpha\hat{\rho}^\beta)_{ba}, \tag{11}$$

$$\mathcal{L}_{P^*P^*V} = \sqrt{2}\beta g_V P_b^*\cdot P_a^{*\dagger}v\cdot\hat{\rho}_{ba} - i2\sqrt{2}\lambda g_V P_b^{*\mu}P_a^{*\nu\dagger}(\partial_\mu\hat{\rho}_\nu - \partial_\nu\hat{\rho}_\mu)_{ba}, \tag{12}$$

$$\mathcal{L}_{PP\sigma} = -2g_sP_bP_b^\dagger\sigma, \tag{13}$$

$$\mathcal{L}_{P^*P^*\sigma} = 2g_sP_b^*\cdot P_b^{*\dagger}\sigma. \tag{14}$$

In the above, $f_\pi = 132$ MeV is the pion decay constant. The coupling constant g was studied by many theoretical approaches, such as quark model [33] and QCD sum rule [36,37]. In our study, we take the experimental result of the CLEO collaboration, $g = 0.59 \pm 0.07 \pm 0.01$, which was extracted from the full width of D^{*+} [38]. For the coupling constants relative to the vector meson exchange, we adopt the values $g_v = 5.8$ and $\beta = 0.9$ which were determined by the vector meson dominance mechanism, and $\lambda = 0.56$ GeV^{-1} which was obtained by matching the form factor predicted by the effective theory approach with that obtained by the light cone sum rule and the lattice QCD simulation [39,40]. The coupling constant for the scalar meson exchange is $g_s = g_\pi/(2\sqrt{6})$ [10] with $g_\pi = 3.73$. We take the masses of the heavy mesons and the exchanged light mesons from PDG [41] and summarize them in Table III.

B. The derivation of the effective potentials

Using the Lagrangians given in Eqs. (8)–(14), one can easily deduce the effective potentials in the momentum space. Taking into account the structure effect of the heavy mesons, we introduce a monopole form factor

$$F(q) = \frac{\Lambda^2 - m_{ex}^2}{\Lambda^2 - q^2} \tag{15}$$

TABLE III. The masses of the heavy mesons and the exchanged light mesons taken from the PDG [41]. In our study, we keep the isospin symmetry. For the isospin multiplet, we use the averaged mass in our study.

Heavy mesons	Mass (MeV)	Exchanged mesons	Mass (MeV)
$D^\pm$	1869.60	$\pi^\pm$	139.57
D^0	1864.83	π^0	134.98
$D^{*\pm}$	2010.25	η	547.85
D^{*0}	2006.96	ρ	775.49
$D_s^\pm$	1968.47	ω	782.65
$D_s^{*\pm}$	2112.3	ϕ	1019.46
B^*	5325.1	σ	600
$B^\pm$	5279.17	$K^\pm$	493.67
B^0	5279.50	K^0	497.61
B_s^0	5366.3	$K^{*\pm}$	891.66
B_s^*	5415.4	K^{*0}	895.94

at each vertex. Here, Λ is the cutoff parameter and $m_{\rm ex}$ is the mass of the exchanged meson.

We need to emphasize that there is an alternative approach to deduce the effective potential just shown in Refs. [42,43], where they refuse to introduce the form factor due to the lack of knowledge of form factors. Here, one can also regularize the divergence of the potential at short distance from a renormalization viewpoint. For the detailed information of the renormalization approach, the interested readers can refer to Refs. [42,43], where the coordinate space renormalization, i.e., boundary conditions, is adopted.

Making Fourier transformation

$$V(r) = \frac{1}{(2\pi)^3}\int d\mathbf{q}^3 e^{-i\mathbf{q}\cdot\mathbf{r}} V(\mathbf{q}) F^2(\mathbf{q}), \tag{16}$$

one can obtain the effective potentials in the coordinate space. In Eqs. (18)–(31), we list the specific expressions of the effective subpotentials which are flavor independent. The effective potential used in our calculation is the product of the flavor-independent subpotentials and the isospin-dependent coefficients which are summarized in the Appendix. The flavor-independent subpotentials are

$$V^a_\sigma(r) = -g_s^2 H_0(\Lambda, q_0, m_\sigma, r), \tag{17}$$

$$V^a_v(r) = \frac{\beta^2 g_V^2}{2} H_0(\Lambda, q_0, m_v, r), \tag{18}$$

for the process $PP \longrightarrow PP$,

$$V^b_{p/\sigma/v}(r) = 0, \tag{19}$$

for the scattering process $PP \longrightarrow PP^*$,

$$V^c_p(r) = \frac{g^2}{f_\pi^2}\Big[H_3(\Lambda, q_0, m_p, r) T(\boldsymbol{\epsilon}_3^\dagger, \boldsymbol{\epsilon}_4^\dagger) + \frac{1}{3} H_1(\Lambda, q_0, m_p, r) S(\boldsymbol{\epsilon}_3^\dagger, \boldsymbol{\epsilon}_4^\dagger)\Big], \tag{20}$$

$$V^c_v(r) = -2\lambda^2 g_V^2\Big[H_3(\Lambda, q_0, m_v, r) T(\boldsymbol{\epsilon}_3^\dagger, \boldsymbol{\epsilon}_4^\dagger) - \frac{2}{3} H_1(\Lambda, q_0, m_v, r) S(\boldsymbol{\epsilon}_3^\dagger, \boldsymbol{\epsilon}_4^\dagger)\Big], \tag{21}$$

for the scattering process $PP \longrightarrow P^*P^*$,

$$V^d_\sigma(r) = -g_s^2 H_0(\Lambda, q_0, m_\sigma, r) S(\boldsymbol{\epsilon}_4^\dagger, \boldsymbol{\epsilon}_2), \tag{22}$$

$$V^d_v(r) = \frac{\beta^2 g_V^2}{2} H_0(\Lambda, q_0, m_v, r) S(\boldsymbol{\epsilon}_4^\dagger, \boldsymbol{\epsilon}_2), \tag{23}$$

for the scattering process $PP^* \longrightarrow PP^*$,

$$V^e_\pi(r) = \frac{g^2}{f_\pi^2}\Big[M_3(\Lambda, q_0, m_\pi, r) T(\boldsymbol{\epsilon}_3^\dagger, \boldsymbol{\epsilon}_2) + \frac{1}{3} M_1(\Lambda, q_0, m_\pi, r) S(\boldsymbol{\epsilon}_3^\dagger, \boldsymbol{\epsilon}_2)\Big], \tag{24}$$

$$V^e_{\pi/\eta/K}(r) = \frac{g^2}{f_\pi^2}\Big[H_3(\Lambda, q_0, m_{\pi/\eta/K}, r) T(\boldsymbol{\epsilon}_3^\dagger, \boldsymbol{\epsilon}_2) + \frac{1}{3} H_1(\Lambda, q_0, m_{\pi/\eta/K}, r) S(\boldsymbol{\epsilon}_3^\dagger, \boldsymbol{\epsilon}_2)\Big] \tag{25}$$

$$V^e_v(r) = -2\lambda^2 g_V^2\Big[H_3(\Lambda, q_0, m_v, r) T(\boldsymbol{\epsilon}_3^\dagger, \boldsymbol{\epsilon}_2) - \frac{2}{3} H_1(\Lambda, q_0, m_v, r) S(\boldsymbol{\epsilon}_3^\dagger, \boldsymbol{\epsilon}_2)\Big], \tag{26}$$

for the scattering process $PP^* \longrightarrow P^*P$,

$$V^f_p(r) = \frac{g^2}{f_\pi^2}\Big[H_3(\Lambda, q_0, m_p, r) T(\boldsymbol{\epsilon}_3^\dagger, i\boldsymbol{\epsilon}_4^\dagger \times \boldsymbol{\epsilon}_2) + \frac{1}{3} H_1(\Lambda, q_0, m_p, r) S(\boldsymbol{\epsilon}_3^\dagger, i\boldsymbol{\epsilon}_4^\dagger \times \boldsymbol{\epsilon}_2)\Big], \tag{27}$$

$$V^f_v(r) = 2\lambda^2 g_V^2\Big\{H_3(\Lambda, q_0, m_v, r)[T(i\boldsymbol{\epsilon}_3^\dagger \times \boldsymbol{\epsilon}_4^\dagger, \boldsymbol{\epsilon}_2) - T(i\boldsymbol{\epsilon}_3^\dagger \times \boldsymbol{\epsilon}_2^\dagger, \boldsymbol{\epsilon}_4^\dagger)] + \frac{1}{3} H_1(\Lambda, q_0, m_v, r) \times [S(i\boldsymbol{\epsilon}_3^\dagger \times \boldsymbol{\epsilon}_4^\dagger, \boldsymbol{\epsilon}_2) - S(i\boldsymbol{\epsilon}_3^\dagger \times \boldsymbol{\epsilon}_2^\dagger, \boldsymbol{\epsilon}_4^\dagger)]\Big\}, \tag{28}$$

for the scattering process $PP^* \longrightarrow P^*P^*$, and

$$V^h_p(r) = \frac{g^2}{f_\pi^2}\Big[H_3(\Lambda, q_0, m_p, r) T(i\boldsymbol{\epsilon}_3^\dagger \times \boldsymbol{\epsilon}_1, i\boldsymbol{\epsilon}_4^\dagger \times \boldsymbol{\epsilon}_2) + \frac{1}{3} H_1(\Lambda, q_0, m_p, r) S(i\boldsymbol{\epsilon}_3^\dagger \times \boldsymbol{\epsilon}_1, i\boldsymbol{\epsilon}_4^\dagger \times \boldsymbol{\epsilon}_2)\Big], \tag{29}$$

$$V^h_\sigma(r) = -g_s^2 H_0(\Lambda, q_0, m_\sigma, r) C(i\boldsymbol{\epsilon}_3^\dagger \times \boldsymbol{\epsilon}_1, i\boldsymbol{\epsilon}_4^\dagger \times \boldsymbol{\epsilon}_2), \tag{30}$$

$$V^h_v(r) = \frac{\beta^2 g_V^2}{2} H_0(\Lambda, q_0, m_v, r) C(i\boldsymbol{\epsilon}_3^\dagger \times \boldsymbol{\epsilon}_1, i\boldsymbol{\epsilon}_4^\dagger \times \boldsymbol{\epsilon}_2) - 2\lambda^2 g_V^2\Big[H_3(\Lambda, q_0, m_v, r) T(i\boldsymbol{\epsilon}_3^\dagger \times \boldsymbol{\epsilon}_1, i\boldsymbol{\epsilon}_4^\dagger \times \boldsymbol{\epsilon}_2) - \frac{2}{3} H_1(\Lambda, q_0, m_v, r) S(i\boldsymbol{\epsilon}_3^\dagger \times \boldsymbol{\epsilon}_1, i\boldsymbol{\epsilon}_4^\dagger \times \boldsymbol{\epsilon}_2)\Big], \tag{31}$$

for the scattering process $P^*P^* \longrightarrow P^*P^*$. To obtain the effective potentials $V^g(r)$ for the process $P^*P \longrightarrow P^*P^*$, one just needs to make the following changes:

$$\begin{aligned}
&\boldsymbol{\epsilon}_3^\dagger \to \boldsymbol{\epsilon}_4^\dagger, \qquad i\boldsymbol{\epsilon}_4^\dagger \times \boldsymbol{\epsilon}_2 \to i\boldsymbol{\epsilon}_3^+ \times \boldsymbol{\epsilon}_1^\dagger,\\
&\boldsymbol{\epsilon}_2 \to \boldsymbol{\epsilon}_1, \qquad i\boldsymbol{\epsilon}_3^\dagger \times \boldsymbol{\epsilon}_4^\dagger \to i\boldsymbol{\epsilon}_4^\dagger \times \boldsymbol{\epsilon}_3^\dagger,\\
&\boldsymbol{\epsilon}_4^\dagger \to \boldsymbol{\epsilon}_3^\dagger, \qquad i\boldsymbol{\epsilon}_3^\dagger \times \boldsymbol{\epsilon}_2 \to i\boldsymbol{\epsilon}_4^\dagger \times \boldsymbol{\epsilon}_1,
\end{aligned} \tag{32}$$

in Eqs. (27) and (28). Functions H_0, H_1, H_3, M_1, and M_3 are given in the Appendix. Operator C, the generalized tensor operator T and spin-spin operator S are defined as

$$C(a, b) = ab, \tag{33}$$

$$T(\boldsymbol{a}, \boldsymbol{b}) = \frac{3\boldsymbol{a}\cdot\boldsymbol{r}\boldsymbol{b}\cdot\boldsymbol{r}}{r^2} - \boldsymbol{a}\cdot\boldsymbol{b}, \tag{34}$$

$$S(\boldsymbol{a}, \boldsymbol{b}) = \boldsymbol{a}\cdot\boldsymbol{b}. \tag{35}$$

Due to the large mass gap between the mesons $D(D^0, D^+)$, D_s^+, $D^*(D^{*0}, D^{*+})$ and D_s^{*+} (similarly, in the bottom sector), it is necessary to adopt the nonzero time component of the transferred momentum for some scattering processes. We present the q_0s used in our calculation in the Appendix. Notice that $m_{D^*} - m_D > m_\pi$ leads to the complex potential for the scattering process $DD^* \to D^*D$, and we take its real part which has an oscillation form, see Eq. (24).

III. NUMERICAL RESULTS

Using the potentials given in the Sec. II B, we solve the coupled-channel Schrödinger equation and summarize the

TABLE IV. The numerical results for the $D^{(*)}D^{(*)}$ system. "$***$" means the corresponding state does not exist due to symmetry while "$\cdots$" means there does not exist binding energy with the cutoff parameter less than 3.0 GeV. The binding energies for the states $D^{(*)}D^{(*)}[I(J^p) = 0(1^+)]$ and $D^{(*)}D^{(*)}[I(J^P) = 1(1^+)]$ are relative to the threshold of DD^* while that of the state $D^{(*)}D^{(*)}[I(J^P) = 1(0^+)]$ is relative to the DD threshold.

			$D^{(*)}D^{(*)}$							
I	J^P		OPE				OBE			
	0^+			$***$				$***$		
		Λ (GeV)	1.05	1.10	1.15	1.20	0.95	1.00	1.05	1.10
		B.E. (MeV)	1.24	4.63	11.02	20.98	0.47	5.44	18.72	42.82
		M (MeV)	3874.61	3871.22	3864.83	3854.87	3875.38	3870.41	3857.13	3833.03
		$r_{\rm rms}$ (fm)	3.11	1.68	1.12	0.84	4.46	1.58	0.91	0.64
0	1^+	P_1 (%)	96.39	92.71	88.22	83.34	97.97	92.94	85.64	77.88
		P_2 (%)	0.73	0.72	0.57	0.42	0.58	0.55	0.32	0.15
		P_3 (%)	2.79	6.45	11.07	16.11	1.41	6.42	13.97	21.91
		P_4 (%)	0.08	0.13	0.14	0.13	0.04	0.09	0.08	0.05
	2^+		$\cdots$	$\cdots$	$\cdots$	$\cdots$	$\cdots$	$\cdots$	$\cdots$	$\cdots$
		Λ (GeV)	$\cdots$	$\cdots$	$\cdots$	$\cdots$	2.64	2.66	2.68	2.70
		B.E. (MeV)	$\cdots$	$\cdots$	$\cdots$	$\cdots$	4.29	12.63	23.30	35.75
		M (MeV)	$\cdots$	$\cdots$	$\cdots$	$\cdots$	3730.17	3721.83	3711.16	3698.71
	0^+	$r_{\rm rms}$ (fm)	$\cdots$	$\cdots$	$\cdots$	$\cdots$	1.38	0.79	0.58	0.48
		P_1 (%)	$\cdots$	$\cdots$	$\cdots$	$\cdots$	91.47	88.26	86.25	84.80
		P_2 (%)	$\cdots$	$\cdots$	$\cdots$	$\cdots$	8.46	11.64	13.63	15.07
		P_3 (%)	$\cdots$	$\cdots$	$\cdots$	$\cdots$	0.07	0.10	0.12	0.13
		Λ (GeV)	$\cdots$	$\cdots$	$\cdots$	$\cdots$	2.48	2.50	2.52	2.54
		B.E. (MeV)	$\cdots$	$\cdots$	$\cdots$	$\cdots$	0.27	3.82	9.79	17.39
		M (MeV)	$\cdots$	$\cdots$	$\cdots$	$\cdots$	3875.58	3872.03	3866.06	3858.46
1	1^+	$r_{\rm rms}$ (fm)	$\cdots$	$\cdots$	$\cdots$	$\cdots$	5.81	1.47	0.91	0.69
		P_2 (%)	$\cdots$	$\cdots$	$\cdots$	$\cdots$	99.92	99.90	99.90	99.90
		P_3 (%)	$\cdots$	$\cdots$	$\cdots$	$\cdots$	0.06	0.06	0.04	0.04
		P_4 (%)	$\cdots$	$\cdots$	$\cdots$	$\cdots$	0.02	0.05	0.06	0.06
		Λ (GeV)	$\cdots$	$\cdots$	$\cdots$	$\cdots$	2.48	2.50	2.52	2.54
		B.E. (MeV)	$\cdots$	$\cdots$	$\cdots$	$\cdots$	2.95	8.86	16.51	25.54
		M (MeV)	$\cdots$	$\cdots$	$\cdots$	$\cdots$	4014.29	4008.38	4000.73	3991.70
	2^+	$r_{\rm rms}$ (fm)	$\cdots$	$\cdots$	$\cdots$	$\cdots$	1.61	0.92	0.68	0.56
		P_1 (%)	$\cdots$	$\cdots$	$\cdots$		99.93	99.94	99.95	99.95
		P_2 (%)	$\cdots$	$\cdots$	$\cdots$	$\cdots$	0.01	0.01	0.01	0.00
		P_3 (%)	$\cdots$	$\cdots$	$\cdots$	$\cdots$	0.06	0.05	0.04	0.04

TABLE V. The numerical results for the $\bar{B}^{(*)}\bar{B}^{(*)}$ system. "$***$" means the corresponding state does not exist due to the symmetry. The binding energies of the states $\bar{B}^{(*)}\bar{B}^{(*)}[I(J^P) = 0(1^+)]$, $\bar{B}^{(*)}\bar{B}^{(*)}[I(J^P) = 0(2^+)]$, and $\bar{B}^{(*)}\bar{B}^{(*)}[I(J^P) = 1(1^+)]$ are relative to the $\bar{B}\bar{B}^*$ threshold while that of the state $\bar{B}^{(*)}\bar{B}^{(*)}[I(J^P) = 1(0^+)]$ is relative to the $\bar{B}\,\bar{B}$ threshold.

			$\bar{B}^{(*)}\bar{B}^{(*)}$							
I	J^P		OPE				OBE			
	0^+			$***$				$***$		
		Λ (GeV)	1.25	1.30	1.40	1.50	1.10	1.15	1.20	1.25
		B.E. (MeV)	0.36	1.14	4.10	9.44	0.19	1.56	5.20	13.71
		M (MeV)	10604.08	10603.30	10600.34	10595.00	10604.25	10602.88	10599.24	10590.73
	1^+	$r_{\rm rms}$ (fm)	3.60	2.25	1.40	1.04	4.86	1.99	1.26	0.86
		P_1 (%)	94.29	91.83	89.03	83.18	96.66	94.17	92.34	86.54
		P_2 (%)	4.16	5.66	7.01	7.10	2.61	4.04	3.54	1.96
0		P_3 (%)	0.77	1.20	1.74	1.89	0.36	0.97	3.14	10.79
		P_4 (%)	0.78	1.30	2.21	2.83	0.37	0.82	0.98	0.72
		Λ (GeV)	2.88	2.90	2.94	2.96	1.66	1.68	1.70	1.72
		B.E. (MeV)	2.75	5.18	10.38	13.15	8.30	28.01	49.89	73.89
	2^+	$r_{\rm rms}$ fm	0.72	0.68	0.63	0.61	0.39	0.35	0.32	0.31
		M (MeV)	10601.69	10599.26	10594.06	10591.29	10596.14	10576.43	10554.55	10530.55
		P_1 (%)	61.15	60.47	59.43	59.01	57.82	55.86	54.69	53.88
		P_2 (%)	38.85	39.53	40.57	40.99	42.18	44.14	45.31	46.12
		Λ (GeV)	1.70	1.75	1.80	1.90	1.74	1.76	1.78	1.80
		B.E. (MeV)	1.05	2.53	4.70	11.29	2.24	8.19	15.67	24.33
		M (MeV)	10557.63	10556.15	10553.98	10547.39	10556.44	10550.49	10543.01	10534.35
	0^+	$r_{\rm rms}$ (fm)	2.07	1.40	1.07	0.75	1.03	0.55	0.42	0.36
		P_1 (%)	95.35	92.82	90.29	85.46	87.27	83.59	81.81	80.66
		P_2 (%)	2.02	3.20	2.42	6.84	12.54	16.26	18.07	19.25
		P_3 (%)	2.63	3.98	5.28	7.70	0.19	0.15	0.11	0.08
		Λ (GeV)	1.40	1.50	1.60	1.70	1.66	1.68	1.70	1.72
		B.E. (MeV)	0.83	1.89	6.46	11.80	0.55	3.72	8.29	13.92
		M (MeV)	10603.61	10601.55	10597.98	10592.64	10603.89	10600.72	10596.15	10590.52
1	1^+	$r_{\rm rms}$ (fm)	2.36	1.38	1.00	0.80	2.26	0.85	0.59	0.48
		P_1 (%)	96.59	94.40	92.43	90.63	99.24	99.34	99.51	99.64
		P_2 (%)	1.62	2.35	2.88	3.29	0.41	0.30	0.20	0.14
		P_3 (%)	1.79	3.25	4.69	6.08	0.34	0.36	0.29	0.22
		Λ (GeV)	1.80	1.90	2.00	2.10	1.70	1.72	1.74	1.76
		B.E. (MeV)	2.25	4.74	8.38	13.35	7.88	13.63	20.36	28.01
		M (MeV)	10647.95	10645.46	10641.82	10636.85	10642.32	10636.57	10629.84	10622.19
	2^+	$r_{\rm rms}$	1.48	1.08	0.85	0.71	0.59	0.47	0.41	0.36
		P_1 (%)	95.73	94.86	94.19	93.66	99.70	99.80	99.86	99.91
		P_2 (%)	0.72	0.87	0.97	1.06	0.05	0.03	0.02	0.01
		P_3 (%)	3.55	4.27	4.83	5.28	0.25	0.17	0.12	0.08

numerical results which include the binding energy (B.E.), the system mass (M), the root-mean-square radius ($r_{\rm rms}$) and the probability of the individual channel (P_i) in Tables IV, V, VII, VIII, IX, and X.

In our study, only the cutoff is a free parameter. However, due to the lack of the experimental data, one cannot determine the cutoff exactly. Thus, it is very difficult to draw definite conclusions. Luckily the one-boson-exchange potential model is very successful to describe the deuteron with the cutoff in the range $0.8 < \Lambda < 1.5$ GeV. Following the study of the deuteron with the same formalism and taking into account the mass difference between the heavy meson and the nucleon, we take the range of the cutoff to be $0.9\ {\rm GeV} < \Lambda < 2.5\ {\rm GeV}$. However, this choice is a little arbitrary to some extent. We sincerely hope that in the near future there will be enough experimental data with which one can determine the cutoff exactly.

Besides, we also consider the stability of the results when we draw our conclusions.

A. The numerical results for systems with strangeness $S = 0$

For the systems with strangeness $S = 0$, in order to highlight the role of the long-range pion exchange in the formation of the loosely bound state, we first give the numerical results with the pion-exchange potential alone,

TABLE VI. The numerical results for the $D^{(*)}\bar{B}^{(*)}$ system. "$\cdots$" means we obtain no binding solutions for the corresponding state with the cutoff parameter less than 3.0 GeV. The binding energies of the states $D^{(*)}\bar{B}^{(*)}[I(J^P) = 0(0^+)]$ and $D^{(*)}\bar{B}^{(*)}[I(J^P) = 1(0^+)]$ are relative to the $D\bar{B}^*$ threshold while those of the states $D^{(*)}\bar{B}^{(*)}[I(J^P) = 0(1^+)]$ and $D^{(*)}\bar{B}^{(*)}[I(J^P) = 1(1^+)]$ are relative to the $D\bar{B}$ threshold.

			$D^{(*)}\bar{B}^{(*)}$							
I	J^P		OPE				OBE			
		Λ (GeV)	1.08	1.12	1.16	1.20	1.00	1.02	1.04	1.06
		B.E. (MeV)	0.42	5.13	15.54	31.35	1.92	6.84	15.25	27.16
		M (MeV)	7146.15	7141.15	7131.03	7115.22	7144.65	7139.73	7131.32	7119.41
	0^+	$r_{\rm rms}$ (fm)	4.23	1.27	0.75	0.55	2.07	1.14	0.78	0.61
		P_1 (%)	95.32	82.45	69.99	60.03	91.21	82.14	72.93	64.72
		P_2 (%)	4.39	17.00	29.51	39.59	8.47	17.49	26.75	35.03
		P_3 (%)	0.28	0.55	0.50	0.38	0.32	0.37	0.32	0.25
		Λ (GeV)	2.05	2.10	2.15	2.20	1.65	1.70	1.75	1.80
		B.E. (MeV)	1.21	2.44	4.13	6.30	0.44	2.83	10.75	30.86
		M (MeV)	7191.12	7189.89	7188.20	7186.03	7191.89	7189.50	7181.58	7161.47
		$r_{\rm rms}$ (fm)	2.75	2.02	1.63	1.37	4.37	1.89	1.05	0.65
		P_1 (%)	96.81	95.59	94.42	93.31	98.72	95.20	84.46	65.15
0	1^+	P_2 (%)	0.00	0.01	0.01	0.01	0.00	0.00	0.01	0.01
		P_3 (%)	0.22	0.30	0.38	0.46	0.26	1.49	5.96	13.96
		P_4 (%)	1.10	1.51	1.90	2.26	0.28	0.53	0.58	0.34
		P_5 (%)	0.29	0.40	0.50	0.59	0.39	2.08	8.23	20.08
		P_6 (%)	0.38	0.52	0.67	0.80	0.09	0.20	0.24	0.16
		P_7 (%)	1.20	1.67	2.13	2.56	0.26	0.50	0.52	0.29
		Λ (GeV)	2.10	2.15	2.20	2.30	1.90	1.95	2.00	2.10
		B.E. (MeV)	0.80	1.31	1.97	3.83	0.63	0.87	1.14	1.79
		M (MeV)	7332.92	7332.41	7331.75	7329.89	7333.09	7332.85	7332.58	7331.93
	2^+	$r_{\rm rms}$ (fm)	3.35	2.71	2.27	1.73	3.79	3.29	2.93	2.43
		P_1 (%)	94.14	92.83	91.58	89.27	96.83	96.41	96.03	95.36
		P_2 (%)	0.25	0.29	0.33	0.38	0.20	0.22	0.24	0.28
		P_3 (%)	5.60	6.88	8.09	10.35	2.97	3.36	3.73	4.36
		Λ (GeV)	2.60	2.70	2.80	2.90	2.22	2.24	2.26	2.28
		B.E. (MeV)	0.14	2.56	8.27	17.53	0.62	6.64	15.45	26.01
		M (MeV)	7146.43	7144.01	7138.30	7129.04	7145.95	7139.93	7131.12	7120.56
	0^+	$r_{\rm rms}$ (fm)	7.05	1.78	1.04	0.75	3.05	0.87	0.57	0.45
		P_1 (%)	98.68	94.88	90.98	87.27	94.14	87.90	85.29	83.65
		P_2 (%)	0.54	2.39	4.36	6.32	5.83	12.05	14.65	16.29
		P_3 (%)	0.66	2.73	4.66	6.41	0.03	0.05	0.06	0.06
		Λ (GeV)	2.55	2.60	2.65	2.70	$\cdots$	$\cdots$	$\cdots$	$\cdots$
		B.E. (MeV)	0.94	2.43	4.67	7.67	$\cdots$	$\cdots$	$\cdots$	$\cdots$
		M (MeV)	7191.39	7189.90	7187.66	7184.66	$\cdots$	$\cdots$	$\cdots$	$\cdots$
		$r_{\rm rms}$ (fm)	2.87	1.83	1.35	1.08	$\cdots$	$\cdots$	$\cdots$	$\cdots$
		P_1 (%)	96.13	93.82	91.53	89.31	$\cdots$	$\cdots$	$\cdots$	$\cdots$
1	1^+	P_2 (%)	0.00	0.01	0.01	0.01	$\cdots$	$\cdots$	$\cdots$	$\cdots$
		P_3 (%)	0.99	1.64	2.33	3.03	$\cdots$	$\cdots$	$\cdots$	$\cdots$
		P_4 (%)	0.70	1.09	1.45	1.77	$\cdots$	$\cdots$	$\cdots$	$\cdots$
		P_5 (%)	0.92	1.48	2.03	2.57	$\cdots$	$\cdots$	$\cdots$	$\cdots$
		P_6 (%)	0.26	0.41	0.54	0.66	$\cdots$	$\cdots$	$\cdots$	$\cdots$
		P_7 (%)	0.99	1.56	2.12	2.66	$\cdots$	$\cdots$	$\cdots$	$\cdots$
		Λ (GeV)	2.80	2.85	2.90	2.95	2.10	2.12	2.14	2.16
		B.E. (MeV)	0.49	1.11	2.00	3.17	0.44	4.64	10.86	18.45
		M (MeV)	7333.23	7332.61	7331.72	7330.55	7333.28	7329.08	7322.86	7315.27
	2^+	$r_{\rm rms}$ (fm)	3.80	2.57	1.95	1.58	3.51	1.03	0.68	0.54
		P_1 (%)	98.57	98.03	97.56	97.15	99.86	99.89	99.93	99.95
		P_2 (%)	0.24	0.33	0.40	0.47	0.02	0.02	0.01	0.01
		P_3 (%)	1.20	1.65	2.04	2.38	0.12	0.09	0.06	0.04

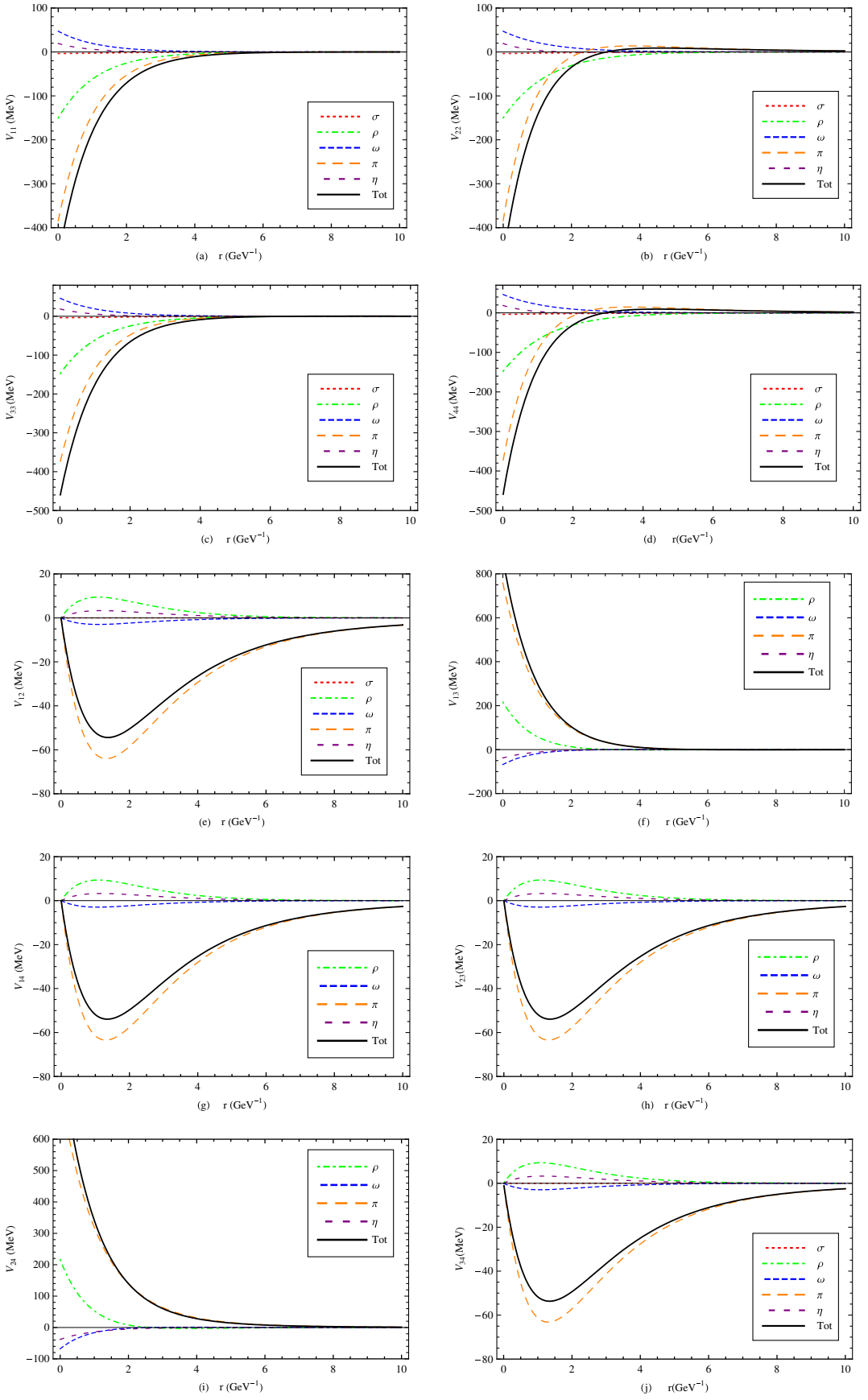

FIG. 1 (color online). The effective potentials for the state $D^{(*)}D^{(*)}[I(J^P) = 0(1^+)]$ with cutoff = 1.00 GeV.

which are marked with OPE, and then with the heavier eta, sigma, rho, and omega exchanges as well as the pion exchange, which are marked with OBE, see Tables IV, V, and VI.

1. $D^{(*)}D^{(*)}$

The state $D^{(*)}D^{(*)}[I(J^P) = 0(0^+)]$ is forbidden because the present boson system should satisfy the boson-Einstein statistic. However, the state $D^{(*)}D^{(*)}[I(J^P) = 0(1^+)]$ is very interesting. Using the long-range pion exchange potential, we obtain a loosely bound state with a reasonable cutoff. For our present $D^{(*)}D^{(*)}[I(J^P) = 0(1^+)]$ state, with the cutoff parameter fixed larger than 1.05 GeV, the long-range pion exchange is strong enough to form the loosely bound state. If we set the cutoff parameter to be 1.05 GeV, the binding energy relative to the DD^* threshold is 1.24 MeV and the corresponding root-mean-square radius is 3.11 fm which is comparable to the size of the deuteron (about 2.0 fm). The dominant channel is $[DD^*]_-(^3S_1)$, with a probability 96.39%. With such a large mass gap (about 140 MeV) between the threshold of DD^* and that of D^*D^*, the contribution of the state $D^*D^*(^3S_1)$ is 2.79%. However, the probability of the D wave is around 1%. When we tune the cutoff to be 1.20 GeV, the binding energy is 20.98 MeV and the root-mean-square radius changes into 0.84 fm. When we use the one-boson-exchange potential, we notice that the binding becomes deeper. For example, if the cutoff is fixed at 1.10 GeV, the binding energy is 4.63 MeV with OPE potential. However, it changes into 42.82 GeV with the OBE potential for the same cutoff, see Table IV. We also plot the potentials in Fig. 1. From the potentials, one can see that the heavier rho and omega exchanges cancel each other significantly, which can be easily understood since for the isospin-zero system the isospin factor of ρ is -3 while that of ω is 1. From the potentials V_{11}, V_{22}, V_{33}, and V_{44} of Fig. 1, one can also see clearly that the total potential is below the π-exchange potential and the contributions of the η and σ exchanges are very small. This implies that the total potential of the ρ and ω exchanges is helpful to strengthen the binding. We note that the OBE potentials deduced by introducing the form factor generate spurious deeply bound states [42]. In order to fix this problem, we also plot the wave function in Fig. 2 from which one can see that there is no node except the origin. In other words, it is really a ground state.

To see the effect of the σ, ρ, and ω exchanges, we turn off the contributions of the π and η exchanges and do the calculation again. We obtain a loosely bound state with binding energy being 0.78 MeV and root-mean-square radius being 3.74 fm when the cutoff parameter is fixed to be 1.44 GeV, which is much larger than 1.05 GeV used in the one-pion-exchange case with almost the same binding energy. Again, this means that the contribution of the long-range pion exchange is larger than that of the heavier vector meson exchange in the formation of the loosely

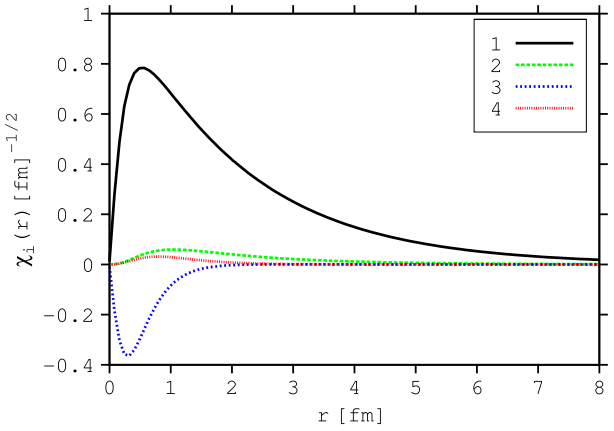

FIG. 2 (color online). The wave function $[r\psi(r)]$ of the $D^{(*)}D^{(*)}$ system with strangeness 0 and $I(J^P) = 0(1^+)$ when the cutoff parameter is fixed to be 1.0 GeV.

bound $D^{(*)}D^{(*)}[I(J^P) = 0(1+)]$ state. This is different from the conclusion of the paper [44] in which the authors studied the charmed meson-charmed antimeson systems with an effective field theory. In their power counting, the leading order contribution arises from the four-meson contact interaction and the one-pion-exchange interaction is perturbative. The interested reader can refer to the paper [44] for detailed information. With the numerical results and the analysis above, the state $D^{(*)}D^{(*)}[I(J^P) = 0(1^+)]$ might be a good molecule candidate.

We should mention that in the calculation of the $X(3872)$ one also obtained a bound $D\bar{D}^*$ state with quantum numbers $I(J^{PC}) = 0(1^{++})$ using the OPE potential [45,46]. One may be confused since the difference between the potential of the DD^* system and that of the $D\bar{D}^*$ system is the G-parity of the exchanged meson while the pion has an odd G-parity. Actually, the isosinglet $D\bar{D}^*$ system has two C-parity states, one with even C-parity ($C = +$) and the other with odd C-parity ($C = -$). And, the interaction of our present DD^* system relates to that of the odd C-parity but not the even C-parity $D\bar{D}^*$ state via the G-parity rule.

We obtain no binding solutions for the state $D^{(*)}D^{(*)}[I(J^P) = 0(2^+)]$ even if we tune the cutoff parameter as high as 3.0 GeV. It seems that the present meson-exchange model does not support the state $D^{(*)}D^{(*)}[I(J^P) = 0(2^+)]$ to be a molecule.

For the state $D^{(*)}D^{(*)}[I(J^P) = 1(0^+)]$, with the cutoff less than 3.0 GeV, the long-range pion exchange is not sufficient to form the bound state. However, when we add the heavier eta, sigma, rho, and omega exchanges and tune the cutoff to be 2.64 MeV, a bound state with mass 3730.17 MeV appears. The binding energy relative to the DD threshold is 2.64 MeV and the corresponding root-mean-square radius is 1.38 fm. The channel $DD(^1S_0)$ with a probability of 91.47% dominates this state. The probability of the channel $D^*D^*(^5D_0)$ is very small, only 0.07%.

Just as the $J^P = 0^+$ case, with the pion-exchange potential alone we obtain no binding solutions for the state $D^{(*)}D^{(*)}[I(J^P) = 1(1^+)]$ with the cutoff parameter less than 3.0 GeV. When we use the OBE potential and tune the cutoff to be 2.48 GeV, we obtain a bound $D^{(*)}D^{(*)}[I(J^P) = 1(1^+)]$ state with mass 3875.58 MeV. The binding energy relative to the DD^* threshold is 0.27 MeV and the corresponding root-mean-square radius is 5.81 fm. The dominant channel is $[DD^*]_+(^3S_1)$, with a probability of 99.92%.

For the state $D^{(*)}D^{(*)}[I(J^P) = 1(2^+)]$, it is necessary to mention that there are five channels $DD(^1D_2)$, $[DD^*]_+ \times (^3D_2)$, $D^*D^*(^5S_2)$, $D^*D^*(^1D_2)$, and $D^*D^*(^5D_2)$, with the quantum numbers $I(J^P) = 1(2^+)$. If we consider all the five channels, with the OBE potential we obtain a bound state with the cutoff parameter fixed to be 2.84 GeV. The binding energy relative to the DD threshold is 12.93 MeV. Surprisingly, the corresponding root-mean-square radius is as small as 0.22 fm. The dominant channel is $D^*D^*(^5S_2)$, with a probability of 99.5%. However, the probability of the channel $DD(^1D_2)$ is as small as 0.04%, which tells us that this is not a loosely bound DD state but a deeply bound D^*D^* state. With so tight a bound state, the present meson-exchange model does not work. Therefore, we omit the channels $DD(^3D_2)$ and $[DD^*]_+(^3D_2)$ and keep the three D^*D^* channels. With the pion-exchange potential we fail to obtain a bound state with the cutoff parameter less than 3.0 GeV. However, when we use the OBE potential and tune the cutoff to be 2.48 GeV, we obtain a bound state with mass 4014.29 MeV. The binding energy is 2.95 MeV and the corresponding root-mean-square radius is 1.61 fm. The channel $D^*D^*(^5S_2)$ with a probability of 99.93% dominates this state.

The three states $D^{(*)}D^{(*)}[I(J^P) = 1(0^+), 1(1^+), 1(2^+)]$ do not form molecules due to the large cutoff in the present meson-exchange model.

2. $\bar{B}^{(*)}\bar{B}^{(*)}$

With the heavy quark flavor symmetry, the potentials for the $\bar{B}^{(*)}\bar{B}^{(*)}$ system are similar to those for the DD system. The main difference between the two systems is that the reduced mass of the $\bar{B}^{(*)}\bar{B}^{(*)}$ system is much larger than that of the $D^{(*)}D^{(*)}$ system. We summarize our numerical results of the $\bar{B}^{(*)}\bar{B}^{(*)}$ system in Table V.

Similar to the charmed state $D^{(*)}D^{(*)}[I(J^P) = 0(1^+)]$, the bottomed state $\bar{B}^{(*)}\bar{B}^{(*)}[I(J^P) = 0(1^+)]$ is also very interesting. The long-range pion exchange is strong enough to form the loosely bound $\bar{B}^{(*)}\bar{B}^{(*)}[I(J^P) = 0(1^+)]$ state with the cutoff larger than 1.25 GeV. If we tune the cutoff to be 1.30 GeV, the binding energy is 1.14 MeV and the corresponding root-mean-square radius is 2.25 fm. The channel $[\bar{B}\bar{B}^*]_-(^3S_1)$ with a probability of 91.83% dominates this state. The probability of the D wave is 6.96%, see Table V. When we use the OBE potential, the binding becomes tighter as expected, which is similar to its charmed partner $D^{(*)}D^{(*)}[I(J^P) = 0(1^+)]$. The numerical results suggest that the state $\bar{B}^{(*)}\bar{B}^{(*)}[I(J^P) = 0(1^+)]$ seems to be a good molecule candidate.

Different from its charmed partner, $\bar{B}^{(*)}\bar{B}^{(*)}[I(J^P) = 0(2^+)]$ can form a bound state with the pion-exchange potential if the cutoff is tuned larger than 2.88 GeV. When we set the cutoff to be 2.88 GeV, the binding energy is 2.75 MeV, and correspondingly, the root-mean-square radius is 0.72 fm. When we use the OBE potential, we obtain the binding solutions with a smaller but more reasonable cutoff. Unfortunately, the binding solutions depend very sensitively on the cutoff parameter. When tune the cutoff from 1.66 to 1.72 GeV, the binding energy changes from 8.30 to 73.89 MeV. Despite the *reasonable* cutoff, we cannot draw a definite conclusion about the state $\bar{B}^{(*)}\bar{B}^{(*)}[I(J^P) = 0(2^+)]$ because of the strong dependence of the results on the cutoff.

The pion-exchange alone is also sufficient to form the loosely bound $\bar{B}^{(*)}\bar{B}^{(*)}[I(J^P) = 1(0^+)]$ state with the cutoff larger than 1.70 GeV. When we tune the cutoff from 1.70 to 1.90 GeV, the binding energy increases from 1.05 to 11.29 MeV, and correspondingly, the root-mean-square radius decreases from 2.07 to 0.75 fm. The dominant channel is $\bar{B}\,\bar{B}(^1S_0)$, with a probability of 95.35%–90.29%. The probability of the channel $D^*D^*(^5D_0)$ is 1.79%–4.69%. Actually, two pseudoscalar D mesons cannot interact with each other via exchanging a pion. Therefore, the binding solutions totally come from the coupled-channel effect, just as in the $\Lambda_Q\Lambda_Q$ case [47,48]. When we add the contributions of the heavier eta, sigma, rho, and omega exchanges, the results change little, which implies that the eta, sigma, rho, and omega exchanges cancel with each other significantly. Although the results depend a little sensitively on the cutoff, the state $\bar{B}^{(*)}\bar{B}^{(*)}[I(J^P) = 1(0^+)]$ might also be a molecule candidate.

The state $\bar{B}^{(*)}\bar{B}^{(*)}[I(J^P) = 1(1^+)]$ is also an interesting one. When we tune the cutoff between 1.40 and 1.70 GeV, we also obtain a loosely bound state with the OPE potential. The binding energy is 0.83–11.80 MeV and the corresponding root-mean-square radius is 2.36–0.80 fm. The dominant channel is $[\bar{B}\bar{B}^*]_+(^3S_1)$, with a probability of 96.59%–90.63%. Different from the isospin singlet case, when we use the OBE potential the binding becomes shallower. For example, with the OPE potential the binding energy is 11.80 MeV if the cutoff is set to be 1.70 MeV while with the OBE potential it is 8.29 MeV for the same cutoff, see Table V. The present numerical results indicate that the state $\bar{B}^{(*)}\bar{B}^{(*)}[I(J^P) = 1(1^+)]$ might be a good molecule candidate.

With the same reason as for the charmed case, we only keep the three channels $\bar{B}^*\bar{B}^*(^5S_2)$, $\bar{B}^*\bar{B}^*(^1D_2)$, and $\bar{B}^*\bar{B}^*(^5D_2)$ for the state $\bar{B}^{(*)}\bar{B}^{(*)}[I(J^P) = 0(2^+)]$. With the pion-exchange potential, when we tune the cutoff between

1.80 and 2.10 GeV, we obtain a loosely bound state with binding energy 2.25–13.35 MeV and root-mean-square radius 1.48–0.71 fm. The dominant channel is $\bar{B}^*\bar{B}^*(^5S_2)$, with a probability of 95.73%–93.66%. When we use the OBE potential and tune the cutoff from 1.70 to 1.76 GeV, the binding energy changes into 7.88–28.01 MeV, and correspondingly, the root-mean-square radius changes into 0.59–0.36 fm. Similar to the $I(J^P) = 1(0^+)$ case, the state $\bar{B}^{(*)}\bar{B}^{(*)}[I(J^P) = 1(2^+)]$ might also be a molecule candidate.

3. $D^{(*)}\bar{B}^{(*)}$

The small binding energy and large root-mean-square radius with reasonable cutoff parameter makes the state $D^{(*)}\bar{B}^{(*)}[I(J^P) = 0(0^+)]$ very interesting. With the OPE potential, when we fix the cutoff between 1.08 and 1.20 GeV, we obtain a loosely bound state with binding energy 0.423–1.35 MeV and root-mean-square radius 4.23–0.55 fm. The dominant channel is $D\bar{B}(^1S_0)$, with a probability of 95.32%–60.03%. The probability of the channel $D^*\bar{B}^*(^5D_0)$ is very small as expected, see Table VI. When we add the contributions of the heavier eta, sigma, rho, and omega exchanges, the binding energy changes by tens of MeV. It seems that the state $D^{(*)}\bar{B}^{(*)}[I(J^P) = 0(0^+)]$ might be a molecule candidate, but not a good one because the results depend a little sensitively on the cutoff.

When the cutoff is tuned larger than 2.05 GeV, the long-range pion exchange is strong enough to form the loosely bound $D^{(*)}\bar{B}^{(*)}[I(J^P) = 0(1^+)]$ state. If we set the cutoff between 2.05 and 2.20 GeV, the binding energy relative to the $D\bar{B}^*$ threshold is 1.21–6.30 MeV while the root-mean-square radius is 2.75–1.37 fm. The dominant channel is $D\bar{B}^*(^3S_1)$, with a probability of 96.81%–93.31%. When we add the contributions of the heavier eta, sigma, rho, and omega exchanges, we obtain a loosely bound $D^{(*)}\bar{B}^{(*)}[I(J^P) = 0(1^+)]$ state with a reasonable cutoff 1.65–1.80 GeV. If we set the cutoff parameter to be 1.70 GeV, the binding energy is 2.83 MeV and the root-mean-square radius is 1.89 fm which is comparable to the size of the deuteron (about 2.0 fm). The channel $D\bar{B}^*(^3S_1)$ with a probability of 95.20% dominates this state. However, the contribution of the D wave is small, less than 5.0%. With the numerical results we predict the state $D^{(*)}\bar{B}^{(*)}[I(J^P) = 0(1^+)]$ to be a molecule.

With the same reason as for the state $\bar{B}^{(*)}\bar{B}^{(*)}[I(J^P) = 0(2^+)]$, we omit the channels $D\bar{B}(^1D_2)$, $D\bar{B}^*(^3D_2)$, and $D^*\bar{B}(^3D_2)$ for the state $D^{(*)}\bar{B}^{(*)}[I(J^P) = 0(2^+)]$. Since the amplitudes of the channel $D^*\bar{B}^*(^3D_2)$ scattering into the other channels are zero, we also omit this channel in our study. With the OPE potential, when we set the cutoff between 2.10 and 2.30 GeV, we obtain a bound $D^{(*)}\bar{B}^{(*)}[I(J^P) = 0(2^+)]$ state, with binding energy 0.80–3.83 fm and root-mean-square radius 3.35–1.73 fm. The channel $D^*\bar{B}^*(^5S_2)$ provides a dominant contribution, 94.14%–89.27%. When we use the OBE potential, the binding energy is 0.63–1.79 MeV and the root-mean-square radius is 3.70–2.43 fm for the cutoff between 1.90 and 2.10 GeV. Such a loosely bound state with weak dependence of the binding solutions on the cutoff parameter is particularly interesting. Thus the present meson-exchange approach favors the state $D^{(*)}\bar{B}[I(J^P) = 0(2^+)]$ to be a good molecule candidate.

For the state $D^{(*)}\bar{B}^{(*)}[I(J^P) = 1(0^+)]$, if we tune the cutoff parameter larger than 2.60 GeV, the OPE potential is sufficient to form the $D^{(*)}\bar{B}^{(*)}[I(J^P) = 1(0^+)]$ bound state. When we fix the cutoff parameter between 2.60 and 2.90 Gev, the binding energy is 0.14–17.53 fm and the corresponding root-mean-square radius is 7.05–0.75 fm. The dominant channel is $D\bar{B}(^1S_0)$, with a probability of 98.68%–87.27%. When we use the OBE potential, we obtain binding solutions with a cutoff parameter larger than 2.22 GeV, see Table VI. The state $D^{(*)}\bar{B}^{(*)}[I(J^P) = 1(0^+)]$ might also be a molecule candidate.

For the state $D^{(*)}\bar{B}^{(*)}[I(J^P) = 1(1^+)]$, when we tune the cutoff parameter larger than 2.55 GeV, we obtain binding solutions with the OPE potential. If we set the cutoff parameter to be 2.60 GeV, the binding energy relative to the $D\bar{B}^*$ threshold is 2.43 MeV and the corresponding root-mean-square radius is 1.83 fm. However, when we add the heavier eta, sigma, rho, and omega exchanges, we obtain no binding solutions with the cutoff parameter less than 3.0 GeV. It seems that the present meson-exchange approach does not support the state $D^{(*)}\bar{B}^{(*)}[I(J^P) = 1(1^+)]$ to be a molecule.

For the state $D^{(*)}\bar{B}^{(*)}[I(J^P) = 1(2^+)]$, when we tune the cutoff parameter as large as 2.80 GeV, we obtain binding solutions with the OPE potential. If we set the cutoff parameter to be 2.90 GeV, the binding energy is 2.00 MeV and the corresponding root-mean-square radius is 1.95 fm. The dominant channel is $D^*\bar{B}^*(^5S_2)$, with a probability of 97.56%. The probability of the D wave is 2.44%. When we use the OBE potential, we obtain binding solutions with a smaller cutoff, see Table VI. If we tune the cutoff to be 2.10 GeV, the binding energy is 0.44 MeV. Similar to the $I(J^P) = 1(0^+)$ case, the state $D^{(*)}\bar{B}^{(*)}[I(J^P) = 1(2^+)]$ might also be a molecule.

B. The results for the systems with strangeness $S = 1$

For the systems with strangeness $S = 1$, there does not exist the long-range pion exchange, but there are heavier eta, sigma, K and K^* exchanges. We summarize our numerical results in Table VII for $(DD)_s$ and $(\bar{B}\,\bar{B})_s$ and in Table VIII for $(D\bar{B})_s$.

1. $(D^{(*)}D^{(*)})_s$ and $(\bar{B}^{(*)}\bar{B}^{(*)})_s$

When we fix the cutoff parameter between 2.70 and 2.76 GeV, we obtain a bound state of $(D^{(*)}D^{(*)})_s \times [J^P = 0^+]$ with mass between 3832.06 and 3802.15 MeV

TABLE VII. The numerical results for the $(D^{(*)}D^{(*)})_s/(\bar{B}^{(*)}\bar{B}^{(*)})_s$ systems. The binding energy of the state $(D^{(*)}D^{(*)})_s/(\bar{B}^{(*)}\bar{B}^{(*)})_s \times [J^P = 0^+]$ is relative to the DD_s threshold while that of the state $(D^{(*)}D^{(*)})_s/(\bar{B}^{(*)}\bar{B}^{(*)})_s[J^P = 1^+]$ is relative to the $D^*D_s/\bar{B}^*\bar{B}_s$ threshold.

J^P		$(D^{(*)}D^{(*)})_s$				$(\bar{B}^{(*)}\bar{B}^{(*)})_s$			
	Λ (GeV)	2.70	2.72	2.74	2.76	1.82	1.84	1.86	1.88
	B.E. (MeV)	3.66	11.31	21.47	33.57	0.56	5.27	12.08	20.32
	M (MeV)	3832.06	3824.41	3814.25	3802.15	10645.08	10640.37	10633.56	10625.32
0^+	$r_{\rm rms}$ (fm)	1.53	0.85	0.62	0.50	2.28	0.71	0.48	0.39
	P_1 (%)	92.85	89.58	87.42	85.82	92.78	86.34	83.69	82.06
	P_2 (%)	7.10	10.34	12.49	14.07	7.12	13.54	16.21	17.86
	P_3 (%)	0.05	0.08	0.09	0.11	0.10	0.12	0.10	0.07
	Λ (GeV)	1.44	1.46	1.48	1.50	1.10	1.12	1.14	1.16
	B.E. (MeV)	5.43	10.19	16.31	23.84	0.67	3.21	7.17	12.52
	M (MeV)	3971.68	3966.92	3960.80	3953.27	10690.73	10688.19	10684.23	10678.88
	$r_{\rm rms}$ (fm)	1.36	1.05	0.87	0.74	2.19	1.10	0.81	0.66
	P_1 (%)	45.80	47.33	47.81	47.85	24.53	36.91	41.11	42.75
1^+	P_2 (%)	0.14	0.15	0.15	0.14	0.22	0.32	0.34	0.33
	P_3 (%)	51.31	48.83	47.40	46.41	72.97	58.66	52.92	49.87
	P_4 (%)	0.12	0.13	0.13	0.13	0.36	0.42	0.40	0.36
	P_5 (%)	2.61	3.54	4.49	5.44	1.83	3.55	5.09	6.54
	P_6 (%)	0.02	0.02	0.02	0.02	0.09	0.13	0.14	0.15
	P_7 (%)	0.00	0.00	0.00	0.00	0.01	0.00	0.00	0.00
	Λ (GeV)	2.54	2.56	2.58	2.60	1.76	1.78	1.80	1.82
	B.E. (MeV)	1.54	6.59	13.67	22.29	0.92	4.74	9.98	16.34
	M (MeV)	4119.38	4114.33	4107.25	4098.63	10739.60	10735.82	10730.52	10724.26
2^+	$r_{\rm rms}$ (fm)	2.28	1.07	0.75	0.60	1.70	0.75	0.54	0.44
	P_1 (%)	99.98	99.97	99.97	99.97	99.76	99.79	99.85	99.85
	P_2 (%)	0.00	0.00	0.00	0.00	0.04	0.03	0.02	0.02
	P_3 (%)	0.02	0.03	0.03	0.03	0.20	0.17	0.13	0.10

and a large root-mean-square radius 1.53–0.50 fm. The dominant channel is $DD_s(^1S_0)$ with a probability of 92.85%–85.82% and the second largest channel $D^*D^*(^1S_0)$ contributes 7.10%–14.07%. The contribution of the channel $D^*D_s^*(^5D_0)$ is very small, only 0.05%–0.11%. Now the cutoff parameter is 2.70 GeV which is twice as large as that for the deuteron (0.8–1.5 GeV [49]). Besides, the binding solutions depend sensitively on the cutoff. It seems that the present meson-exchange approach does not support the state $(D^{(*)}D^{(*)})_s[J^P = 0^+]$ to be a molecule candidate.

In the corresponding bottom sector, we also obtain a bound state of $(\bar{B}^{(*)}\bar{B}^{(*)})_s[J^P = 0^+]$ with a smaller and more reasonable cutoff, 1.82–1.88 GeV. This can be easily understood since the mass of the bottomed mesons are much larger than those of the charmed mesons and the effective potentials for the two systems are similar. When we tune the cutoff to be 1.82 GeV, the binding energy is 0.56 GeV and the root-mean-square is 2.28 fm which is comparable to that of the deuteron (about 2.0 fm), see Table VII. The numerical results indicate that the state $(\bar{B}^{(*)}\bar{B}^{(*)})_s[J^P = 0^+]$ might be a molecule candidate although not a good one.

For the charmed state $(D^{(*)}D^{(*)})_s[J^P = 1^+]$, when we set the cutoff to be 1.44 GeV, the binding energy is 5.43 MeV and the root-mean-square radius is 1.36 fm. The closeness of the thresholds for DD_s^* and D^*D_s makes the channels $DD_s^*(^3S_1)$ and $D^*D_s(^3S_1)$ provide the comparable and main contributions, 45.80% for $DD_s^*(^3S_1)$ and 51.31% for $D^*D_s(^3S_1)$. The D-wave channel $D^*D_s^*(^3D_1)$ and $D^*D_s^*$ provide almost vanishing contributions, 0.02% for $D^*D_s^*(3D_1)$ and 0.00% for $D^*D_s^*(^5D_1)$. This is because of the large mass gap between $D^*D_s^*$ and D^*D_s and the strong repulsive interaction coming from the centrifugal potential of the D wave. The numerical results suggest that the state $(D^{(*)}D^{(*)})_s[J^P = 1^+]$ might also be a molecule candidate. The results of the state $(\bar{B}^{(*)}\bar{B}^{(*)})_s[J^P = 1^+])$ are similar to those of the state $(D^{(*)}D^{(*)})_s[J^P = 1^+]$, but with smaller cutoff 1.10–1.16 GeV and weaker dependence on the cutoff, see Table VII. Thus the state $(\bar{B}^{(*)}\bar{B}^{(*)})_s[J^P = 1^+])$ seems to be a good molecule candidate.

For the state $(D^{(*)}D^{(*)})_s[J^P = 2^+]$, we obtain a bound state with binding energy 1.54–22.29 MeV when we tune the cutoff to be 2.54–2.60 GeV. The root-mean square

TABLE VIII. The numerical results for the $(D^{(*)}\bar{B}^{(*)})_s$ system. The binding energy of the state $(D^{(*)}\bar{B}^{(*)})_s[J^P = 0^+]$ is relative to the $D\bar{B}_s$ threshold while those of the states $(D^{(*)}\bar{B}^{(*)})_s[J^P = 1^+]$ and $(D^{(*)}\bar{B}^{(*)})_s[J^P = 2^+]$ correspond to the thresholds of $D\bar{B}_s^*$ and $D^*\bar{B}_s^*$ respectively.

J^P		$(D^{(*)}\bar{B}^{(*)})_s$			
0^+	Λ (GeV)	1.28	1.30	1.32	1.34
	B.E. (MeV)	6.72	22.10	43.11	68.73
	M (MeV)	7226.81	7211.43	7190.42	7164.80
	$r_{\rm rms}$ (fm)	0.92	0.55	0.43	0.36
	P_1 (%)	50.10	36.04	29.33	25.30
	P_2 (%)	25.66	26.98	25.07	23.02
	P_3 (%)	12.03	18.55	22.96	26.05
	P_4 (%)	12.06	18.30	22.56	25.58
	P_5 (%)	0.07	0.05	0.04	0.03
	P_6 (%)	0.08	0.06	0.04	0.03
1^+	Λ (GeV)	1.24	1.26	1.28	1.30
	B.E. (MeV)	2.50	14.97	32.88	54.86
	M (MeV)	7280.13	7267.66	7249.75	7227.77
	$r_{\rm rms}$ (fm)	1.45	0.63	0.47	0.39
	P_1 (%)	19.11	23.61	22.14	20.40
	P_2 (%)	58.10	35.98	28.14	23.97
	P_3 (%)	4.65	8.04	9.71	10.69
	P_4 (%)	4.63	8.16	9.86	10.80
	P_5 (%)	6.73	11.95	14.87	16.84
	P_6 (%)	6.72	12.21	15.26	17.28
	P_7 (%)	0.00	0.00	0.00	0.00
	P_8 (%)	0.00	0.00	0.00	0.00
	P_9 (%)	0.04	0.03	0.02	0.01
	P_{10}(%)	0.03	0.02	0.02	0.01
2^+	Λ (GeV)	2.20	2.22	2.24	2.26
	B.E. (MeV)	1.23	5.68	12.65	21.29
	M (MeV)	7422.79	7418.34	7411.37	7402.73
	$r_{\rm rms}$ (fm)	2.25	0.95	0.62	0.49
	P_1 (%)	10.90	26.64	36.08	40.94
	P_2 (%)	88.81	73.18	63.83	59.01
	P_3 (%)	0.02	0.01	0.01	0.00
	P_4 (%)	0.01	0.00	0.00	0.00
	P_5 (%)	0.18	0.12	0.06	0.03
	P_6 (%)	0.09	0.05	0.02	0.01

radius is 2.28–0.60 fm. The dominant channel is $D^*D_s^*(^5S_2)$, with a probability of 99.98%. However, the contributions of the D wave are negligible. The numerical results suggest that the present meson-exchange approach does not support $(D^{(*)}D^{(*)})_s[J^P = 2^+]$ to be a molecule due to the large cutoff.

For the state $(\bar{B}^{(*)}\bar{B}^{(*)})_s[J^P = 2^+]$, if we fix the cutoff parameter between 1.76 and 1.82 GeV, the binding energy is 0.92–16.34 MeV and the root-mean-square radius is 1.70–0.44 fm. The dominant channel is $\bar{B}^*\bar{B}_s^*(^5S_2)$ with a probability of 99.76%–99.85%. Such a loosely bound state is very interesting, and it might be a good molecule candidate.

2. $(D^{(*)}\bar{B}^{(*)})_s$

For the state $(D^{(*)}\bar{B}^{(*)})_s[J^P = 0^+]$, if we set the cutoff parameter to be 1.28 GeV, the binding energy is 6.72 MeV and correspondingly, the root-mean-square radius is 0.92 fm. The probability of the channel $D\bar{B}_s(^1S_0)$ is 50.10% while that of the channel $D_s\bar{B}(^1S_0)$ is 25.66%. However, if the binding energy is 68.73 MeV, these two channels provide comparable contributions, 25.30% for $D\bar{B}_s(^1S_0)$ and 23.02% for $D_s\bar{B}(^1S_0)$. Given that the mass gap between $D\bar{B}_s$ and $D_s\bar{B}$ is around 14.5 MeV, for the binding energy comparable to this value, the mass gap plays an important role in the formation of the loosely bound state. However, if the binding energy is as large as 68.73 MeV, which is much larger than the mass gap, the important effect of the mass gap is gone, which is similar to the case of $X(3872)$ [46]. Despite *reasonable* cutoff, we cannot draw a definite conclusion about the state $(D^{(*)}\bar{B}^{(*)})_s \times [J^P = 0^+]$ due to the strong dependence of the results on the cutoff.

It is necessary to mention that there exist fourteen channels for the state $(D^{(*)}\bar{B}^{(*)})_s[J^P = 1^+]$. It is very hard to solve a 14×14 matrix Shrödinger equation. Due to the large mass gap between the threshold of $D^*\bar{B}_s^*$ (or $D_s^*\bar{B}^*$) and that of $D\bar{B}_s^*$ and the strong repulsive interaction coming from the D wave, we expect the channels $D^*\bar{B}_s^*(^3D_1)$, $D^*\bar{B}_s^*(^5D_1)$, $D_s^*\bar{B}^*(^3D_1)$, and $D_s^*\bar{B}^*(^5D_1)$ to provide negligible contributions, which can be clearly seen from the previous calculation. Therefore, we omit these four channels in our calculation. We obtain a bound state of $(D^{(*)}\bar{B}^{(*)})_s[J^P = 1^+]$ with the cutoff larger than 1.24 GeV and the results are similar to those of $(D^{(*)}\bar{B}^{(*)})_s[J^P = 0^+]$, see Table VIII.

For the state $(D^{(*)}\bar{B}^{(*)})_s[J^P = 2^+]$, if the cutoff parameter is fixed to be 2.20 GeV, the binding energy relative to threshold of $D^*\bar{B}_s^*$ is 1.23 MeV and the root-mean-square radius is 2.25 fm. The dominant channel is $D^*\bar{B}_s^*(^5S_2)$, with a probability of 88.81%. The other S-wave channel $D_s^*\bar{B}^*(^5S_2)$ provides the second largest contribution, 10.90%, and the total contribution of the D wave is 0.3%. It seems that the present meson-exchange approach supports $(D^{(*)}\bar{B}^{(*)})_s[J^P = 2^+]$ to be a molecule candidate, but not a good one.

C. The results for the systems with strangeness $S = 2$

For the systems with strangeness $S = 2$, there does not exist the long-range pion exchange, but there are mediate-range sigma and eta exchanges and the short-range phi exchange. We summarize the numerical results for the systems $(D^{(*)}D^{(*)})_{ss}$ and $(\bar{B}^{(*)}\bar{B}^{(*)})_{ss}$ in Table IX and for the system $(D^{(*)}\bar{B}^{(*)})_{ss}$ in Table X.

TABLE IX. The numerical results for the $(D^{(*)}D^{(*)})_{ss}/(\bar{B}^{(*)}\bar{B}^{(*)})_{ss}$ systems. The binding energy of the state $(D^{(*)}D^{(*)})_{ss}/(\bar{B}^{(*)}\bar{B}^{(*)})_{ss}[J^P = 0^+]$ corresponds to the $D_sD_s/\bar{B}_s\bar{B}_s$ threshold while that of the state $(D^{(*)}D^{(*)})_{ss}/(\bar{B}^{(*)}\bar{B}^{(*)})_{ss}$ corresponds to the threshold of $D_sD_s^*/\bar{B}_s\bar{B}_s^*$.

J^P		$(D^{(*)}D^{(*)})_{ss}$				$(\bar{B}^{(*)}\bar{B}^{(*)})_{ss}$			
	Λ (GeV)	2.76	2.78	2.80	2.82	1.90	1.92	1.94	1.96
	B.E. (MeV)	2.43	8.68	17.56	28.53	2.27	6.97	13.30	20.99
	M (MeV)	3934.55	3928.30	3919.42	3908.45	10730.33	10725.63	10719.30	10711.61
0^+	$r_{\rm rms}$ (fm)	1.92	1.00	0.70	0.55	1.17	0.67	0.49	0.40
	P_1 (%)	94.69	91.37	89.04	87.27	90.83	87.05	84.67	83.00
	P_2 (%)	5.29	8.59	10.91	12.68	8.88	12.65	15.05	16.76
	P_3 (%)	0.02	0.03	0.04	0.05	0.29	0.30	0.28	0.24
	Λ (GeV)	2.62	2.64	2.66	2.68	1.82	1.84	1.86	1.88
	B.E. (MeV)	0.41	3.75	9.32	16.57	0.83	3.39	7.16	11.98
	M (MeV)	4080.38	4077.04	4071.47	4064.22	10778.27	10775.71	10771.94	10767.12
1^+	$r_{\rm rms}$ (fm)	4.64	1.49	0.94	0.71	1.95	0.96	0.68	0.54
	P_1 (%)	99.98	99.96	99.96	99.96	99.41	99.29	99.33	99.41
	P_2 (%)	0.01	0.02	0.02	0.01	0.24	0.27	0.24	0.20
	P_3 (%)	0.01	0.02	0.02	0.03	0.35	0.44	0.43	0.39
	Λ (GeV)	2.60	2.62	2.64	2.66	1.82	1.84	1.86	1.88
	B.E. (MeV)	0.86	4.79	10.81	18.46	0.22	2.48	6.24	11.15
	M (MeV)	4223.74	4219.81	4213.79	4206.14	10830.61	10828.32	10824.62	10819.72
2^+	$r_{\rm rms}$ (fm)	3.13	1.29	0.86	0.66	3.86	1.10	0.71	0.55
	P_1 (%)	99.98	99.97	99.98	99.98	99.75	99.61	99.64	99.70
	P_2 (%)	0.00	0.00	0.00	0.00	0.04	0.06	0.05	0.04
	P_3 (%)	0.02	0.02	0.02	0.02	0.21	0.33	0.30	0.26

1. $(D^{(*)}D^{(*)})_{ss}$ and $(\bar{B}^{(*)}\bar{B}^{(*)})_{ss}$

If we fix the cutoff parameter between 2.76 and 2.82 GeV, we obtain a bound state of $(D^{(*)}D^{(*)})_{ss}[J^P = 0^+]$ with binding energy 2.43–28.53 MeV and root-mean-square radius 1.92–0.55 fm. The dominant channel is $D_sD_s(^1S_0)$, with a probability of 94.69%–87.27%. The contribution of the D-wave channel $D_s^*D_s^*(^5D_0)$ is very small as expected, less than 0.1%. In the bottomed sector, we obtain binding solutions with a smaller but more reasonable cutoff 1.90–1.96 GeV. As one can easily read off from Table IX, when we set the cutoff to be 1.90 GeV, the binding energy is 2.27 MeV and the root-mean-square is 1.17 fm. The dominant channel is $\bar{B}_s\bar{B}_s(^1S_0)$, with a probability of 90.83%. However, the D-wave channel $\bar{B}^*\bar{B}^*(^5D_0)$ provides a negligible contribution, 0.29%. Based on the numerical results, the state $\bar{B}_s\bar{B}_s(^1S_0)$ might be a molecule whereas the state $(D^{(*)}D^{(*)})_{ss}[J^P = 0^+]$ might not be.

For the state $(D^{(*)}D^{(*)})_{ss}[J^P = 1^+]$, when we tune the cutoff parameter between 2.62 and 2.68 GeV, we obtain binding energy 0.41–16.57 MeV and root-mean-square radius 4.64–0.71 fm. The dominant channel is $[D_sD_s^*]_+ \times (^3S_1)$, with a probability of 99.98%–99.96%. In the corresponding bottomed case, we obtain a loosely bound state of $(\bar{B}\,\bar{B})_{ss}[J^P = 1^+]$ with binding energy 0.83–11.98 MeV and root-mean-square radius 1.95–0.54 fm when we set the cutoff parameter between 1.82 and 1.88 GeV. Similar to the charmed case, the dominant channel is $[\bar{B}_s\bar{B}_s^*]_+(^3S_1)$, providing a contribution of 99.41%–99.29%. Similar to the $J^P = 0^+$ case, it seems that the state $(B^{(*)}B^{(*)})_{ss}[J^P = 1^+]$ might be a molecule whereas the state $(D^{(*)}D^{(*)})_{ss}[J^P = 1^+]$ might not be.

For the $J^P = 2^+$ case, the results are very similar to those of the $J^P = 1^+$ case, see IX.

2. $(D^{(*)}\bar{B}^{(*)})_{ss}$

For the state $(D^{(*)}\bar{B}^{(*)})_{ss}[J^P = 0^+]$, we obtain binding energy 0.64–21.72 MeV and root-mean-square radius 3.11–0.52 fm with the cutoff parameter fixed between 2.36 and 2.42 GeV. The channel $D_s\bar{B}_s(^1S_0)$ with a probability of 96.05%–86.20% is the dominant channel. The probability of the channel $D_s^*\bar{B}_s^*(^5D_0)$ is very small, about 0.03%, see Table X.

For the state $(D^{(*)}\bar{B}^{(*)})_{ss}[J^P = 1^+]$, when we fix the cutoff parameter between 2.34 and 2.40 GeV we obtain binding energy 1.47–23.41 MeV and corresponding root-mean-square radius 2.02–0.50 fm. The dominant channel is $D_s\bar{B}_s^*(^3S_1)$, with a probability of 93.37%–83.13%. However, the total contribution of the D wave is very small, less than 0.1%, see Table X.

Very similar to the $J^P = 0^+$ case, we obtain a bound state of $(D^{(*)}\bar{B}^{(*)})_{ss}[J^P = 2^+]$ with binding energy 2.98–22.29 MeV and root-mean-square radius 1.35–0.51 fm. The

TABLE X. The numerical results for the $(D^{(*)}\bar{B}^{(*)})_{ss}$ system. The binding energy of the state $(D^{(*)}\bar{B}^{(*)})_{ss}[J^P = 0^+]$ is relative to the threshold of $D_s\bar{B}_s$ while that of the state $(D^{(*)}\bar{B}^{(*)})_{ss} \times [J^P = 1^+]$ corresponds to the $D_s\bar{B}_s^*$ threshold.

J^P		$(D^{(*)}\bar{B}^{(*)})_{ss}$			
	Λ (GeV)	2.36	2.38	2.40	2.42
	B.E. (MeV)	0.64	5.16	12.43	21.72
	M (MeV)	7334.15	7329.63	7322.36	7313.07
0^+	$r_{\rm rms}$ (fm)	3.11	1.06	0.68	0.52
	P_1 (%)	96.05	91.15	88.25	86.20
	P_2 (%)	3.94	8.82	11.72	13.17
	P_3 (%)	0.02	0.03	0.03	0.03
	Λ (GeV)	2.34	2.36	2.38	2.40
	B.E. (MeV)	1.47	6.63	14.13	23.41
	M (MeV)	7382.42	7377.26	7369.76	7360.48
	$r_{\rm rms}$ (fm)	2.02	0.92	0.63	0.50
	P_1 (%)	93.37	88.46	85.36	83.13
1^+	P_2 (%)	0.00	0.00	0.00	0.00
	P_3 (%)	3.85	6.95	9.07	10.69
	P_4 (%)	0.01	0.01	0.01	0.01
	P_5 (%)	2.75	4.55	5.54	6.14
	P_6 (%)	0.00	0.00	0.00	0.00
	P_7 (%)	0.02	0.02	0.02	0.02
	Λ (GeV)	2.26	2.28	2.30	2.32
	B.E. (MeV)	2.98	7.96	14.47	22.29
	M (MeV)	7524.72	7519.74	7513.23	7505.41
2^+	$r_{\rm rms}$ (fm)	1.35	0.82	0.62	0.51
	P_1 (%)	99.93	99.94	99.95	99.96
	P_2 (%)	0.01	0.01	0.01	0.01
	P_3 (%)	0.06	0.05	0.04	0.03

dominant channel is $D_s^*\bar{B}_s^*(^5S_2)$, with a probability of 99.98%. The numerical results indicate that the present meson-exchange approach seems to support all of the three states to be molecule candidates, but not good ones since the results depend a little sensitively on the cutoff.

IV. CONCLUSION

In the present paper, we investigate the possible molecular states composed of two heavy flavor mesons, including $D^{(*)}D^{(*)}$, $\bar{B}^{(*)}\bar{B}^{(*)}$, and $D^{(*)}\bar{B}^{(*)}$ with strangeness $S = 0$, 1, and 2. In our study, we take into account the S-D mixing which plays an important role in the formation of the loosely bound deuteron, and particularly, the coupled-channel effect in the flavor space.

In order to make clear the role of the long-range pion exchange in the formation of the loosely bound states, we give the numerical results with the one-pion-exchange potential for the system with strangeness $S = 0$, as well as the numerical results with the one-boson-exchange potential.

In our study, we notice that for some systems, such as $D^{(*)}D^{(*)}[I(J^P) = 0(1^+)]$, the probability of the D wave is very small. Additionally, the contributions of the D-wave channel with larger threshold are almost negligible for the system with a large mass gap among the thresholds of different channels. We also notice that, when the binding energy is comparable to or even smaller than the mass gap, the effect of the mass gap will be magnified by the small binding energy, which is similar to the $X(3872)$ case [46].

TABLE XI. The summary of our conclusions. "$***$" means the corresponding state does not exist due to symmetry. "$\surd$" ("$\times$") means the corresponding state might (might not) be a molecule. "$\surd\!\!\!/$" denotes that the corresponding state might be a molecule candidate, but not a good one because the results depend a little sensitive on the cutoff. However,"?" means we cannot draw a definite conclusion with the present meson-exchange approach.

Strangeness	Double charm	$I(J^P)$	Status	Double bottom	$I(J^P)$	Status	Charm and bottom	$I(J^P)$	Status
$S = 0$	$D^{(*)}D^{(*)}$	$0(0^+)$	$***$	$\bar{B}^{(*)}\bar{B}^{(*)}$	$0(0^+)$	$***$	$D^{(*)}\bar{B}^{(*)}$	$0(0^+)$	$\surd\!\!\!/$
		$0(1^+)$	$\surd$		$0(1^+)$	$\surd$		$0(1^+)$	$\surd$
		$0(2^+)$	$\times$		$0(2^+)$	?		$0(2^+)$	$\surd$
		$1(0^+)$	$\times$		$1(0^+)$	$\surd\!\!\!/$		$1(0^+)$	$\surd\!\!\!/$
		$1(1^+)$	$\times$		$1(1^+)$	$\surd$		$1(1^+)$	$\times$
		$1(2^+)$	$\times$		$1(2^+)$	$\surd\!\!\!/$		$1(2^+)$	$\surd\!\!\!/$
$S = 1$	$(D^{(*)}D^{(*)})_s$	$\frac{1}{2}(0^+)$	$\times$	$(\bar{B}^{(*)}\bar{B}^{(*)})_s$	$\frac{1}{2}(0^+)$	$\surd\!\!\!/$	$(D^{(*)}\bar{B}^{(*)})_s$	$\frac{1}{2}(0^+)$	?
		$\frac{1}{2}(1^+)$	$\surd\!\!\!/$		$\frac{1}{2}(1^+)$	$\surd$		$\frac{1}{2}(1^+)$	?
		$\frac{1}{2}(2^+)$	$\times$		$\frac{1}{2}(2^+)$	$\surd$		$\frac{1}{2}(2^+)$	$\surd\!\!\!/$
$S = -2$	$(D^{(*)}D^{(*)})_{ss}$	$0(0^+)$	$\times$	$(\bar{B}^{(*)}\bar{B}^{(*)})_{ss}$	$0(0^+)$	$\surd\!\!\!/$	$(D^{(*)}\bar{B}^{(*)})_{ss}$	$0(0^+)$	$\surd\!\!\!/$
		$0(1^+)$	$\times$		$0(1^+)$	$\surd$		$0(1^+)$	$\surd\!\!\!/$
		$0(2^+)$	$\times$		$0(2^+)$	$\surd$		$0(2^+)$	$\surd\!\!\!/$

In the sector with strangeness $S = 0$, our results favor that $D^{(*)}D^{(*)}[I(J^P) = 0(1^+)]$, $\bar{B}^{(*)}\bar{B}^{(*)}[I(J^P) = 0(1^+), 1(1^+)]$, and $D^{(*)}\bar{B}^{(*)}[I(J^P) = 0(1^+), 0(2^+)]$ are good molecule candidates. For these states, the long-range pion exchange is strong enough to form the loosely bound states, and the medium-range eta and sigma exchanges and the short-range rho and omega exchanges are helpful to strengthen the binding. The states $\bar{B}^{(*)}\bar{B}^{(*)}[I(J^P) = 1(0^+), 1(2^+)]$ and $D^{(*)}\bar{B}^{(*)}[I(J^P) = 0(0^+), 1(0^+), 1(2^+)]$ might also be molecules although the results depend a little sensitively on the cutoff. However, it seems that the present meson-exchange approach does not support the states $D^{(*)}D^{(*)}[I(J^P) = 0(2^+), 1(0^+), 1(1^+), 1(2^+)]$ and $D^{(*)}\bar{B}^{(*)}[I(J^P) = 1(1^+)]$ to be molecules. Despite the *reasonable* cutoff, we cannot draw a definite conclusion about the state $\bar{B}^{(*)}\bar{B}^{(*)}[I(J^P) = 0(2^+)]$ due to the strong dependence on the cutoff. Further detailed study with other approaches will be very helpful to settle this issue.

In the $S = 1$ sector, the states $(\bar{B}^{(*)}\bar{B}^{(*)})_s[J^P = 1^+, 2^+]$ might be good molecule candidates. The states $(D^{(*)}D^{(*)})_s[J^P = 1^+]$, $(\bar{B}^{(*)}\bar{B}^{(*)})_s[J^P = 0^+]$, and $(D^{(*)}\bar{B}^{(*)})_s[J^P = 2^+]$ also seem to be molecule candidates, but not good ones because the results depend a little sensitively on the cutoff. With the same reason as for the $S = 0$ case, we cannot draw definite conclusions on the states $(D^{(*)}\bar{B}^{(*)})_s[J^P = 0^+, 1^+]$. However, the present meson-exchange approach does not seem to support states $(D^{(*)}D^{(*)})_s[J^P = 0^+, 2^+]$ to be molecules.

For the $S = 2$ systems, our results suggest that the states $(\bar{B}^{(*)}\bar{B}^{(*)})_{ss}[J^P = 1^+, 2^+]$ might be good molecule candidates whereas the states $(D^{(*)}D^{(*)})_{ss}[J^P = 0^+, 1^+, 2^+]$ might not be molecules. Although the results depend a little sensitively on the cutoff, the states $(\bar{B}^{(*)}\bar{B}^{(*)})_{ss}[J^p = 0^+]$ and $(D^{(*)}\bar{B}^{(*)})_{ss}[J^P = 0^+, 1^+, 2^+]$ might also be molecules. We summarize our conclusions in Table XI.

In Reference [50], the authors also studied the doubly charmed systems within the hidden gauge formalism in a coupled-channel unitary approach. For the D^*D^* systems with $C = 2$, $S = 0$, and $I = 0$, they only obtained a bound state with quantum number $I(J^P) = 0(1^+)$, which is similar to our result. However, the pole appeared at 3969 MeV, which is 100 MeV larger than our result, 3870 MeV. This is because we consider the coupled channel effect of DD^* to D^*D^*. Actually, what we obtain is a DD^* bound state, but not a D^*D^* bound state. For the systems with $C = 2$, $S = 0$, and $I = 1$, both their results and ours indicate that there are no molecule candidates. For the systems with $C = 2$, $S = 1$, and $I = \frac{1}{2}$, they only obtained a bound state with quantum numbers $I(J^P) = \frac{1}{2}(1^+)$. Our results indicate that only the state with $I(J^P) = \frac{1}{2}(1^+)$ might be a molecule candidate, but not an ideal one because the result depends a bit sensitively on the cutoff parameter. For the systems with $C = 2$, $S = 2$, and $I = 0$, they obtained no bound states, neither do we, see Table XI. Our results and those in Ref. [50]are consistent with each other, although these two theoretical frameworks were quite different.

It is very interesting to search for the predicted exotic hadronic molecular states experimentally. These molecular candidates cannot directly fall apart into the corresponding components due to the absence of the phase space. For these molecular states with double charm, they cannot decay into a double charm baryon plus a light baryon. The masses of the lightest doubly charmed baryon and light baryon are 3518 and 938 MeV, respectively, corresponding to Ξ_{cc}^+ and proton as listed in PDG [41]. The mass of the molecular state is around 3850 MeV and much smaller than the sum of the masses of a doubly charmed baryon and a light baryon. Therefore such a decay is kinematically forbidden.

However, the heavy vector meson within the exotic molecular state may decay. The D^* mainly decays to $D\pi$ via strong interaction. It also decays into $D\gamma$. Similarly, D_s^*, B^*, and B_s^* dominantly decay to $D_s\gamma$, $B\gamma$, and $B_s\gamma$ via electromagnetic interaction, respectively. For example, the main decay modes of the exotic double-charm molecular state with one D^* meson are $DD\gamma$ and $DD\pi$. If the molecular candidates contain two heavy pseudoscalar mesons only, they are stable once produced. The D^* meson may also decay via weak interaction. For these exotic molecules with double bottom or both one charm and one bottom, their decay behavior is similar to that of the molecular state with double charm.

The above typical decay modes provide important information to further experimental search. Although very difficult, it is still possible to produce such heavy systems with double bottom or both one charm and one bottom at LHC.

ACKNOWLEDGMENTS

This project was supported by the National Natural Science Foundation of China under Grants No. 11075004, No. 11021092, No. 11261130311, No. 11222547, No. 11175073, and No. 11035006, Ministry of Science and Technology of China (2009CB825200), the Ministry of Education of China (FANEDD under Grant No. 200924, DPFIHE under Grant No. 20090211120029, NCET, the Fundamental Research Funds for the Central Universities), and the Fok Ying-Tong Education Foundation (No. 131006). This work is also supported in part by the DFG and the NSFC through funds provided to the sinogermen CRC 110 "Symmetries and the Emergence of Structure in QCD."

TABLE XII. The isospin-dependent coefficients for the $D^{(*)}D^{(*)}$ and $D^{(*)}\bar{B}^{(*)}$ systems with strangeness $S = 0$. The coefficients of the $\bar{B}^{(*)}\bar{B}^{(*)}$ systems, which are not shown, are similar to those of the $D^{(*)}D^{(*)}$.

$I = 0$	DD	$[DD^*]_-$	$[DD^*]_+$	D^*D^*
DD	$-\frac{3}{2}\rho^a + \frac{1}{2}\omega^a + \sigma^a$			$-\frac{3}{2}\pi^c + \frac{1}{6}\eta^c - \frac{3}{2}\rho^c + \frac{1}{2}\omega^c$
$[DD^*]_-$		$-\frac{3}{2}\rho^d + \frac{1}{2}\omega^d + \sigma^d$		$\frac{1}{\sqrt{2}}(-\frac{3}{2}\pi^f + \frac{1}{6}\eta^f - \frac{3}{2}\rho^f + \frac{1}{2}\omega^f)$
		$-(-\frac{3}{2}\pi^e + \frac{1}{6}\eta^e - \frac{3}{2}\rho^e + \frac{1}{2}\omega^e)$		$-\frac{1}{\sqrt{2}}(-\frac{3}{2}\pi^g + \frac{1}{6}\eta^g - \frac{3}{2}\rho^g + \frac{1}{2}\omega^g)$
$[DD^*]_+$			$-\frac{3}{2}\rho^d + \frac{1}{2}\omega^d + \sigma^d$	$\frac{1}{\sqrt{2}}(-\frac{3}{2}\pi^f + \frac{1}{6}\eta^f - \frac{3}{2}\rho^f + \frac{1}{2}\omega^f)$
			$+(-\frac{3}{2}\pi^e + \frac{1}{6}\eta^e - \frac{3}{2}\rho^e + \frac{1}{2}\omega^e)$	$+\frac{1}{\sqrt{2}}(-\frac{3}{2}\pi^g + \frac{1}{6}\eta^g - \frac{3}{2}\rho^g + \frac{1}{2}\omega^g)$
D^*D^*				$-\frac{3}{2}\pi^h + \frac{1}{6}\eta^h - \frac{3}{2}\rho^h + \frac{1}{2}\omega^h + \sigma^h$
$I = 1$	DD	$[DD^*]_-$	$[DD^*]_+$	D^*D^*
DD	$\frac{1}{2}\rho^a + \frac{1}{2}\omega^a + \sigma^a$			$\frac{1}{2}\pi^c + \frac{1}{6}\eta^c + \frac{1}{2}\rho^c + \frac{1}{2}\omega^c$
$[DD^*]_-$		$\frac{1}{2}\rho^d + \frac{1}{2}\omega^d + \sigma^d$		$\frac{1}{\sqrt{2}}(\frac{1}{2}\pi^f + \frac{1}{6}\eta^f + \frac{1}{2}\rho^f + \frac{1}{2}\omega^f)$
		$-(\frac{1}{2}\pi^e + \frac{1}{6}\eta^e + \frac{1}{2}\rho^e + \frac{1}{2}\omega^e)$		$-\frac{1}{\sqrt{2}}(\frac{1}{2}\pi^g + \frac{1}{6}\eta^g + \frac{1}{2}\rho^g + \frac{1}{2}\omega^g)$
$[DD^*]_+$			$\frac{1}{2}\rho^d + \frac{1}{2}\omega^d + \sigma^d$	$\frac{1}{\sqrt{2}}(\frac{1}{2}\pi^f + \frac{1}{6}\eta^f + \frac{1}{2}\rho^f + \frac{1}{2}\omega^f)$
			$+(\frac{1}{2}\pi^e + \frac{1}{6}\eta^e + \frac{1}{2}\rho^e + \frac{1}{2}\omega^e)$	$+\frac{1}{\sqrt{2}}(\frac{1}{2}\pi^g + \frac{1}{6}\eta^g + \frac{1}{2}\rho^g + \frac{1}{2}\omega^g)$
D^*D^*				$\frac{1}{2}\pi^h + \frac{1}{6}\eta^h + \frac{1}{2}\rho^h + \frac{1}{2}\omega^h + \sigma^h$
$I = 0$	$D\bar{B}$	$D\bar{B}^*$	$D^*\bar{B}$	$D^*\bar{B}^*$
$D\bar{B}$	$-\frac{3}{2}\rho^a + \frac{1}{2}\omega^a + \sigma^a$			$-\frac{3}{2}\pi^c + \frac{1}{6}\eta^c - \frac{3}{2}\rho^c + \frac{1}{2}\omega^c$
$D\bar{B}^*$		$-\frac{3}{2}\rho^d + \frac{1}{2}\omega^d + \sigma^d$	$-\frac{3}{2}\pi^e + \frac{1}{6}\eta^e - \frac{3}{2}\rho^e + \frac{1}{2}\omega^e$	$-\frac{3}{2}\pi^f + \frac{1}{6}\eta^f - \frac{3}{2}\rho^f + \frac{1}{2}\omega^f$
$D^*\bar{B}$			$-\frac{3}{2}\rho^d + \frac{1}{2}\omega^d + \sigma^d$	$-\frac{3}{2}\pi^g + \frac{1}{6}\eta^g - \frac{3}{2}\rho^g + \frac{1}{2}\omega^g$
$D^*\bar{B}^*$				$-\frac{3}{2}\pi^h + \frac{1}{6}\eta^h - \frac{3}{2}\rho^h + \frac{1}{2}\omega^h + \sigma^h$
$I = 1$	$D\bar{B}$	$D\bar{B}^*$	$D^*\bar{B}$	$D^*\bar{B}^*$
$D\bar{B}$	$\frac{1}{2}\rho^a + \frac{1}{2}\omega^a + \sigma^a$			$\frac{1}{2}\pi^c + \frac{1}{6}\eta^c + \frac{1}{2}\rho^c + \frac{1}{2}\omega^c$
$D\bar{B}^*$		$\frac{1}{2}\rho^d + \frac{1}{2}\omega^d + \sigma^d$	$\frac{1}{2}\pi^e + \frac{1}{6}\eta^e + \frac{1}{2}\rho^e + \frac{1}{2}\omega^e$	$\frac{1}{2}\pi^f + \frac{1}{6}\eta^f + \frac{1}{2}\rho^f + \frac{1}{2}\omega^f$
$D^*\bar{B}$			$\frac{1}{2}\rho^d + \frac{1}{2}\omega^d + \sigma^d$	$\frac{1}{2}\pi^g + \frac{1}{6}\eta^g + \frac{1}{2}\rho^g + \frac{1}{2}\omega^g$
$D^*\bar{B}^*$				$\frac{1}{2}\pi^h + \frac{1}{6}\eta^h + \frac{1}{2}\rho^h + \frac{1}{2}\omega^h + \sigma^h$

TABLE XIII. The isospin-dependent coefficients for the $(D^{(*)}D^{(*)})_s$ and $(D^{(*)}\bar{B}^{(*)})_s$ systems with strangeness $S = 1$. The coefficients of the $(\bar{B}^{(*)}\bar{B}^{(*)})_s$ systems, which are not shown, are similar to those of the $(D^{(*)}D^{(*)})_s$.

	DD_s	DD_s^*	D^*D_s	$D^*D_s^*$
DD_s	$\sigma^a + K^{*a}$	0	0	$-\frac{1}{3}\eta^c + K^c + K^{*c}$
DD_s^*		$\sigma^d + K^e + K^{*e}$	$-\frac{1}{3}\eta^e + K^{*d}$	$-\frac{1}{3}\eta^f + K^f + K^{*f}$
D^*D_s			$\sigma^d + K^e + K^{*e}$	$-\frac{1}{3}\eta^g + K^g + K^{*g}$
$D^*D_s^*$				$-\frac{1}{3}\eta^h + \sigma^h + K^h + K^{*h}$

	$D\bar{B}_s$	$D_s\bar{B}$	$D\bar{B}_s^*$	$D_s^*\bar{B}$	$D^*\bar{B}_s$	$D_s\bar{B}^*$	$D^*\bar{B}_s^*$	$D_s^*\bar{B}^*$
$D\bar{B}_s$	σ^a	K^{*a}	0	0	0	0	$-\frac{1}{3}\eta^c$	$K^c + K^{*c}$
$D_s\bar{B}$		σ^a	0	0	0	0	$K^c + K^{*c}$	$-\frac{1}{3}\eta^c$
$D\bar{B}_s^*$			σ^d	$K^e + K^{*e}$	$-\frac{1}{3}\eta^{*e}$	K^{*d}	$-\frac{1}{3}\eta^f$	$K^f + K^{*f}$
$D_s^*\bar{B}$				σ^d	K^{*d}	$-\frac{1}{3}\eta^e$	$K^g + K^{*g}$	$-\frac{1}{3}\eta^g$
$D^*\bar{B}_s$					σ^d	$K^e + K^{*e}$	$-\frac{1}{3}\eta^g$	$K^g + K^{*g}$
$D_s\bar{B}^*$						σ^d	$K^f + K^{*f}$	$-\frac{1}{3}\eta^f$
$D^*\bar{B}_s^*$							$-\frac{1}{3}\eta^h + \sigma^h$	$K^h + K^{*h}$
$D_s^*\bar{B}^*$								$-\frac{1}{3}\eta^h + \sigma^h$

TABLE XIV. The isospin-dependent coefficients for the $(D^{(*)}D^{(*)})_{ss}$ and $(D^{(*)}\bar{B}^{(*)})_{ss}$ systems with strangeness $S=1$. The coefficients of the $(\bar{B}^{(*)}\bar{B}^{(*)})_{ss}$ systems, which are not shown, are similar to those of the $(D^{(*)}D^{(*)})_{ss}$.

$I=1$	D_sD_s	$[D_sD_s^*]_-$	$[D_sD_s^*]_+$	$D_s^*D_s^*$
D_sD_s	$\phi^a+\sigma^a$	0	0	$\frac{2}{3}\eta^c+\phi^c$
$[D_sD_s^*]_-$		$\phi^d+\sigma^d-(\frac{2}{3}\eta^e+\phi^e)$	$\times$	$\frac{1}{\sqrt{2}}(\frac{2}{3}\eta^f+\phi^f)-\frac{1}{\sqrt{2}}(\frac{2}{3}\eta^g+\phi^g)$
$[D_sD_s^*]_+$			$\phi^d+\sigma^d+(\frac{2}{3}\eta^e+\phi^e)$	$\frac{1}{\sqrt{2}}(\frac{2}{3}\eta^f+\phi^f)+\frac{1}{\sqrt{2}}(\frac{2}{3}\eta^g+\phi^g)$
$D_s^*D_s^*$				$\frac{2}{3}\eta^h+\phi^h+\sigma^h$
	$D_s\bar{B}_s$	$D_s\bar{B}_s^*$	$D_s^*\bar{B}_s$	$D_s^*\bar{B}_s^*$
$D_s\bar{B}_s$	$\phi^a+\sigma^a$	0	0	$\frac{2}{3}\eta^c+\phi^c$
$D_s\bar{B}_s^*$		$\phi^d+\sigma^d$	$\frac{2}{3}\eta^e+\phi^e$	$\frac{2}{3}\eta^f+\phi^f$
$D_s^*\bar{B}_s$			$\phi^d+\sigma^d$	$\frac{2}{3}\eta^g+\phi^g$
$D_s^*\bar{B}_s^*$				$\frac{2}{3}\eta^h+\phi^h+\sigma^h$

APPENDIX

The functions H_i etc. are defined as

$$H_0(\Lambda,q_0,m,r)=\frac{u}{4\pi}\left[Y(ur)-\frac{\chi}{u}Y(\chi r)-\frac{r\beta^2}{2u}Y(\chi r)\right],\quad H_1(\Lambda,q_0,m,r)=\frac{u^3}{4\pi}\left[Y(ur)-\frac{\chi}{u}Y(\chi r)-\frac{r\chi^2\beta^2}{2u^3}Y(\chi r)\right],$$
$$H_3(\Lambda,q_0,m,r)=\frac{u^3}{12\pi}\left[Z(ur)-\frac{\chi^3}{u^3}Z(\chi r)-\frac{\chi\beta^2}{2u^3}Z_2(\chi r)\right],\quad M_1(\Lambda,q_0,m,r)=-\frac{u^3}{4\pi}\left\{\frac{1}{\theta r}[\cos(\theta r)-e^{-\chi r}]+\frac{\chi\beta^2}{2\theta^3}e^{-\chi r}\right\},$$
$$M_3(\Lambda,q_0,m,r)=-\frac{u^3}{12\pi}\left\{\left[\cos(\theta r)-\frac{3\sin(\theta r)}{\theta r}-\frac{3\cos(\theta r)}{\theta^2r^2}\right]\frac{1}{\theta r}+\frac{\chi^3}{\theta^3}Z(\chi r)+\frac{\chi\beta^2}{2\theta^3}Z_2(\chi r)\right\},\tag{A1}$$

where

TABLE XV. The time component of the transferred momentum, q_0, used in our calculation. The other values which are not given are zero.

DD		$\bar{B}\bar{B}$		$D\bar{B}$			
Process	q_0	Process	q_0	Process	q_0	Process	q_0
$DD_s\to D_sD$	$m_{D_s}-m_D$	$\bar{B}\bar{B}_s\to\bar{B}_s\bar{B}$	$m_{B_s}-m_B$	$D_s\bar{B}\to D\bar{B}_s$	$\frac{(m_{B_s}^2+m_{D_s}^2)-(m_B^2+m_D^2)}{2(m_D+m_{B_s})}$	$D\bar{B}_s\to D_s\bar{B}$	$\frac{(m_{B_s}^2+m_{D_s}^2)-(m_B^2+m_D^2)}{2(m_D+m_{B_s})}$
$D_sD\to D_s^*D^*$	$\frac{(m_{D_s^*}^2+m_D^2)-(m_{D_s}^2+m_{D^*}^2)}{2(m_{D^*}+m_{D_s^*})}$	$\bar{B}_s\bar{B}\to\bar{B}_s^*\bar{B}^*$	$\frac{(m_{B_s^*}^2+m_B^2)-(m_{B_s}^2+m_{B^*}^2)}{2(m_{B^*}+m_{B_s^*})}$	$D_s\bar{B}\to D_s^*\bar{B}^*$	$\frac{(m_{D_s^*}^2+m_B^2)-(m_{B^*}^2+m_{D_s}^2)}{2(m_{D^*}+m_{B_s^*})}$	$D_s\bar{B}\to D^*\bar{B}_s^*$	$\frac{(m_{B_s^*}^2+m_{D_s}^2)-(m_{D^*}^2+m_B^2)}{2(m_{D^*}+m_{B_s^*})}$
$D_sD\to D^*D_s^*$	$\frac{(m_{D_s^*}^2+m_{D_s}^2)-(m_D^2+m_{D^*}^2)}{2(m_{D^*}+m_{D_s^*})}$	$\bar{B}_s\bar{B}\to\bar{B}^*\bar{B}_s^*$	$\frac{(m_{B_s^*}^2+m_{B_s}^2)-(m_{B^*}^2+m_B^2)}{2(m_{B^*}+m_{B_s^*})}$	$D\bar{B}_s\to D_s^*\bar{B}^*$	$\frac{(m_{D_s^*}^2+m_{B_s}^2)-(m_D^2+m_{B^*}^2)}{2(m_{D_s}+m_{B^*})}$	$D\bar{B}_s\to D^*\bar{B}_s^*$	$\frac{(m_{D^*}^2+m_{B_s}^2)-(m_B^2+m_{D^*}^2)}{2(m_{D^*}+m_{B_s^*})}$
$D_sD^*\to DD_s^*$	$\frac{(m_{D_s^*}^2+m_{D_s}^2)-(m_D^2+m_{D^*}^2)}{2(m_D+m_{D_s^*})}$	$\bar{B}_s\bar{B}^*\to\bar{B}\bar{B}_s^*$	$\frac{(m_{B_s^*}^2+m_{B_s}^2)-(m_B^2+m_{B^*}^2)}{2(m_B+m_{B_s^*})}$	$D_s\bar{B}^*\to D\bar{B}_s^*$	$\frac{(m_{D_s}^2+m_{B_s^*}^2)-(m_D^2+m_{B^*}^2)}{2(m_{D_s}+m_{B^*})}$	$D_s^*\bar{B}\to D^*\bar{B}_s$	$\frac{(m_{D_s^*}^2+m_{B_s}^2)-(m_B^2+m_{D^*}^2)}{2(m_{D^*}+m_{B_s})}$
$DD^*\to D^*D$	$m_{D^*}-m_D$	$\bar{B}\bar{B}^*\to\bar{B}^*\bar{B}$	$m_{B^*}-m_B$	$D\bar{B}^*\to D^*\bar{B}$	$\frac{(m_{D^*}^2-m_{B^*}^2)-(m_D^2+m_B^2)}{2(m_{D^*}+m_B)}$	$D^*\bar{B}\to D\bar{B}^*$	$\frac{(m_{D^*}^2-m_{B^*}^2)-(m_D^2+m_B^2)}{2(m_{D^*}+m_B)}$
$D_sD^*\to D_s^*D$	$\frac{(m_{D_s^*}^2+m_{D^*}^2)-(m_{D_s}^2+m_D^2)}{2(m_{D_s}+m_{D^*})}$	$\bar{B}_s\bar{B}^*\to\bar{B}_s^*\bar{B}$	$\frac{(m_{B_s^*}^2+m_{B^*}^2)-(m_{B_s}^2+m_B^2)}{2(m_{B_s}+m_{B^*})}$	$D_s\bar{B}^*\to D_s^*\bar{B}$	$\frac{(m_{D_s^*}^2+m_{B^*}^2)-(m_{D_s}^2+m_B^2)}{2(m_{D_s^*}+m_B)}$	$D_s^*\bar{B}\to D_s\bar{B}^*$	$\frac{(m_{D_s^*}^2+m_{B^*}^2)-(m_{B_s}^2+m_D^2)}{2(m_{D_s^*}+m_B)}$
$D_sD^*\to D^*D_s$	$m_{D^*}-m_{D_s}$	$\bar{B}_s\bar{B}^*\to\bar{B}^*\bar{B}_s$	$m_{B^*}-m_{B_s}$	$D_s\bar{B}^*\to D^*\bar{B}_s$	$\frac{(m_{B^*}^2+m_{D^*}^2)-(m_{B_s}^2+m_{D_s}^2)}{2(m_{D^*}+m_{B_s^*})}$	$D_s^*\bar{B}\to D\bar{B}_s^*$	$\frac{(m_{D_s^*}^2+m_{B_s^*}^2)-(m_D^2+m_B^2)}{2(m_{D^*}+m_B)}$
$DD_s^*\to D_s^*D$	$m_{D_s^*}-m_D$	$\bar{B}\bar{B}_s^*\to\bar{B}_s^*\bar{B}$	$m_{B_s^*}-m_B$	$D\bar{B}_s^*\to D_s^*\bar{B}$	$\frac{(m_{B_s^*}^2+m_{D^*}^2)-(m_D^2+m_{B^*}^2)}{2(m_{D^*}+m_B)}$	$D^*\bar{B}\to D_s\bar{B}^*$	$\frac{(m_{D^*}^2+m_{B^*}^2)-(m_{D_s}^2+m_B^2)}{2(m_{D_s}+m_{B^*})}$
$DD_s^*\to D^*D_s$	$\frac{(m_{D_s^*}^2+m_{D^*}^2)-(m_{D_s}^2-m_D^2)}{2(m_{D_s}+m_{D^*})}$	$\bar{B}\bar{B}_s^*\to\bar{B}^*\bar{B}_s$	$\frac{(m_{B_s^*}^2+m_{B^*}^2)-(m_B^2+m_{B_s}^2)}{2(m_{B^*}+m_{B_s})}$	$D\bar{B}_s^*\to D^*\bar{B}_s$	$\frac{(m_{B_s^*}^2+m_{D^*}^2)-(m_D^2+m_{B_s}^2)}{2(m_D+m_{B_s^*})}$	$D^*\bar{B}_s\to D\bar{B}_s^*$	$\frac{(m_{D^*}^2+m_{B_s^*}^2)-(m_D^2+m_{B_s}^2)}{2(m_D+m_{B_s^*})}$
$DD^*\to D^*D^*$	$\frac{m_{D^*}^2-m_D^2}{4m_{D^*}}$	$\bar{B}\bar{B}^*\to\bar{B}^*\bar{B}^*$	$\frac{m_{B^*}^2-m_B^2}{4m_{B^*}}$	$D\bar{B}^*\to D^*\bar{B}^*$	$\frac{m_{D^*}^2-m_D^2}{2(m_{D^*}+m_{B^*})}$	$D^*\bar{B}\to D^*\bar{B}^*$	$\frac{m_{B^*}^2-m_B^2}{2(m_{D^*}+m_{B^*})}$
$D_sD^*\to D_s^*D^*$	$\frac{(m_{D_s^*}^2-m_{D_s}^2)}{2(m_{D^*}+m_{D^*})}$	$\bar{B}_s\bar{B}^*\to\bar{B}_s^*\bar{B}^*$	$\frac{m_{B_s^*}^2-m_{B_s}^2}{2(m_{B^*}+m_{B^*})}$	$D_s\bar{B}^*\to D_s^*\bar{B}^*$	$\frac{m_{D_s^*}^2-m_{D_s}^2}{2(m_{D^*}+m_{B^*})}$	$D_s^*\bar{B}\to D_s^*\bar{B}^*$	$\frac{m_{B^*}^2-m_B^2}{2(m_{D_s^*}+m_{B^*})}$
$D_sD^*\to D^*D_s^*$	$\frac{m_{D_s^*}^2+m_{D_s}^2-2m_{D^*}^2}{2(m_{D^*}+m_{D_s^*})}$	$\bar{B}_s\bar{B}^*\to\bar{B}^*\bar{B}_s^*$	$\frac{m_{B_s^*}^2+m_{B_s}^2-2m_{B^*}^2}{2(m_{B^*}+m_{B_s^*})}$	$D_s\bar{B}^*\to D^*\bar{B}_s^*$	$\frac{(m_{D^*}^2+m_{B_s^*}^2)-(m_{D_s}^2+m_{B^*}^2)}{2(m_{D^*}+m_{B_s^*})}$	$D_s^*\bar{B}\to D^*\bar{B}_s^*$	$\frac{(m_{D_s^*}^2+m_{B_s^*}^2)-(m_{D^*}^2+m_B^2)}{2(m_{D^*}+m_{B_s^*})}$
$DD_s^*\to D_s^*D^*$	$\frac{2m_{D_s^*}^2-m_D^2-m_{D^*}^2}{2(m_{D_s^*}+m_{D^*})}$	$\bar{B}\bar{B}_s^*\to\bar{B}_s^*\bar{B}^*$	$\frac{2m_{B_s^*}^2-m_B^2-m_{B^*}^2}{2(m_{B_s^*}+m_{B^*})}$	$D\bar{B}_s^*\to D_s^*\bar{B}^*$	$\frac{(m_{D_s^*}^2+m_{B^*}^2)-(m_D^2+m_{B^*}^2)}{2(m_{D_s^*}+m_{B^*})}$	$D^*\bar{B}_s\to D_s^*\bar{B}^*$	$\frac{(m_{D_s^*}^2+m_{B^*}^2)-(m_{D^*}^2+m_{B^*}^2)}{2(m_{D_s^*}+m_{B^*})}$
$DD_s^*\to D^*D_s^*$	$\frac{m_{D^*}^2-m_D^2}{2(m_{D^*}+m_{D_s^*})}$	$\bar{B}\bar{B}_s^*\to\bar{B}^*\bar{B}_s^*$	$\frac{m_{B^*}^2-m_B^2}{2(m_{B^*}+m_{B_s^*})}$	$D\bar{B}_s^*\to D^*\bar{B}_s^*$	$\frac{m_{D^*}^2-m_D^2}{2(m_{D^*}+m_{B_s^*})}$	$D^*\bar{B}_s\to D^*\bar{B}_s^*$	$\frac{m_{B_s^*}^2-m_{B_s}^2}{2(m_{D^*}+m_{B_s^*})}$
$D_s^*D^*\to D^*D_s^*$	$m_{D_s^*}-m_{D^*}$	$\bar{B}_s^*\bar{B}^*\to\bar{B}^*\bar{B}_s^*$	$m_{B_s^*}-m_{B^*}$	$D_s^*\bar{B}^*\to D^*\bar{B}_s^*$	$\frac{(m_{B_s^*}^2+m_{D_s^*}^2)-(m_{B^*}^2+m_{D^*}^2)}{2(m_{D^*}+m_{B_s^*})}$	$D^*\bar{B}_s^*\to D_s^*\bar{B}^*$	$\frac{(m_{B_s^*}^2+m_{D_s^*}^2)-(m_{B^*}^2+m_{D^*}^2)}{2(m_{D^*}+m_{B_s^*})}$

$$\beta^2 = \Lambda^2 - m^2, \qquad u^2 = m^2 - q_0^2,$$
$$\theta^2 = -(m^2 - q_0^2), \qquad \chi^2 = \Lambda^2 - q_0^2, \tag{A2}$$

and

$$Y(x) = \frac{e^{-x}}{x}, \qquad Z(x) = \left(1 + \frac{3}{x} + \frac{3}{x^2}\right)Y(x),$$
$$Z_1(x) = \left(\frac{1}{x} + \frac{1}{x^2}\right)Y(x), \qquad Z_2(x) = (1+x)Y(x). \tag{A3}$$

Fourier transformation formulas read

$$\frac{1}{u^2 + \boldsymbol{q}^2} \to H_0(\Lambda, q_0, m, r),$$
$$\frac{\boldsymbol{q}^2}{u^2 + \boldsymbol{q}^2} \to -H_1(\Lambda, q_0, m, r),$$
$$\frac{q_i q_j}{u^2 + \boldsymbol{q}^2} \to -H_3(\Lambda, q_0, m, r)k_{ij} - \frac{1}{3}H_1(\Lambda, q_0, m, r)\delta_{ij}, \tag{A4}$$

where $k_{ij} = 3\frac{r_i r_j}{r^2} - \delta_{ij}$.

We summarize the isospin-dependent coefficients in Tables XII, XIII, and XIV and the time component of the transferred momentum used in our calculation in Table XV.

[1] N. A. Tornqvist, arXiv:hep-ph/0308277.
[2] F. E. Close and P. R. Page, Phys. Lett. B **578**, 119 (2004).
[3] E. S. Swanson, Phys. Lett. B **588**, 189 (2004).
[4] N. A. Tornqvist, Phys. Lett. B **590**, 209 (2004).
[5] X. Liu, X.-Q. Zeng, and X.-Q. Li, Phys. Rev. D **72**, 054023 (2005).
[6] S.-L. Zhu, Phys. Lett. B **625**, 212 (2005).
[7] M. T. AlFiky, F. Gabbiani, and A. A. Petrov, Phys. Lett. B **640**, 238 (2006).
[8] Y.-R. Liu, X. Liu, W.-Z. Deng, and S.-L. Zhu, Eur. Phys. J. C **56**, 63 (2008).
[9] X. Liu, Y.-R. Liu, W.-Z. Deng, and S.-L. Zhu, Phys. Rev. D **77**, 034003 (2008).
[10] X. Liu, Y.-R. Liu, W.-Z. Deng, and S.-L. Zhu, Phys. Rev. D **77**, 094015 (2008).
[11] C. E. Thomas and F. E. Close, Phys. Rev. D **78**, 034007 (2008).
[12] S. H. Lee, K. Morita, and M. Nielsen, Phys. Rev. D **78**, 076001 (2008).
[13] F. Close and C. Downum, Phys. Rev. Lett. **102**, 242003 (2009).
[14] G.-J. Ding, Phys. Rev. D **79**, 014001 (2009).
[15] G.-J. Ding, J.-F. Liu, and M.-L. Yan, Phys. Rev. D **79**, 054005 (2009).
[16] X. Liu, Z.-G. Luo, Y.-R. Liu, and S.-L. Zhu, Eur. Phys. J. C **61**, 411 (2009).
[17] X. Liu and S.-L. Zhu, Phys. Rev. D **80**, 017502 (2009).
[18] Y.-R. Liu and Z.-Y. Zhang, Phys. Rev. C **79**, 035206 (2009).
[19] S. H. Lee, K. Morita, and M. Nielsen, Nucl. Phys. **A815**, 29 (2009).
[20] P. Ortega, J. Segovia, D. Entem, and F. Fernandez, AIP Conf. Proc. **1257**, 331 (2010).
[21] S. Ohkoda, Y. Yamaguchi, S. Yasui, K. Sudoh, and A. Hosaka, Phys. Rev. D **86**, 014004 (2012).
[22] S. Ohkoda, Y. Yamaguchi, S. Yasui, K. Sudoh, and A. Hosaka, arXiv:1209.0144.
[23] F. Aceti, R. Molina, and E. Oset, Proc. Sci., QNP2012 (2012) 072.
[24] M. B. Voloshin and L. B. Okun, JETP Lett. **23**, 333 (1976).
[25] A. De Rujula, H. Georgi, and S. L. Glashow, Phys. Rev. Lett. **38**, 317 (1977).
[26] N. A. Tornqvist, Nuovo Cimento Soc. Ital. Fis. A **107**, 2471 (1994).
[27] N. A. Tornqvist, Z. Phys. C **61**, 525 (1994).
[28] M. Mattson *et al.* (SELEX Collaboration), Phys. Rev. Lett. **89**, 112001 (2002).
[29] A. Ocherashvili *et al.* (SELEX Collaboration), Phys. Lett. B **628**, 18 (2005).
[30] B. Aubert *et al.* (*BABAR* Collaboration), Phys. Rev. D **74**, 011103 (2006).
[31] R. Chistov *et al.* (BELLE Collaboration), Phys. Rev. Lett. **97**, 162001 (2006).
[32] M. B. Wise, Phys. Rev. D **45**, R2188 (1992).
[33] A. F. Falk and M. E. Luke, Phys. Lett. B **292**, 119 (1992).
[34] B. Grinstein, E. E. Jenkins, A. V. Manohar, M. J. Savage, and M. B. Wise, Nucl. Phys. **B380**, 369 (1992).
[35] R. Casalbuoni, A. Deandrea, N. Di Bartolomeo, R. Gatto, F. Feruglio, and G. Nardulli, Phys. Rep. **281**, 145 (1997).
[36] Y.-B. Dai and S.-L. Zhu, Eur. Phys. J. C **6**, 307 (1999).
[37] F. Navarra, M. Nielsen, M. Bracco, M. Chiapparini, and C. Schat, Phys. Lett. B **489**, 319 (2000).
[38] S. Ahmed *et al.* (CLEO Collaboration), Phys. Rev. Lett. **87**, 251801 (2001).
[39] C. Isola, M. Ladisa, G. Nardulli, and P. Santorelli, Phys. Rev. D **68**, 114001 (2003).
[40] M. Bando, T. Kugo, and K. Yamawaki, Phys. Rep. **164**, 217 (1988).
[41] K. Nakamura and P. D. Group, J. Phys. G **37**, 075021 (2010).
[42] A. Calle Cordon and E. Ruiz Arriola, Phys. Rev. C **81**, 044002 (2010).
[43] D. Gamermann, J. Nieves, E. Oset, and E. Ruiz Arriola, Phys. Rev. D **81**, 014029 (2010).
[44] J. Nieves and M. P. Valderrama, Phys. Rev. D **86**, 056004 (2012).
[45] I. W. Lee, A. Faessler, T. Gutsche, and V. E. Lyubovitskij, Phys. Rev. D **80**, 094005 (2009).
[46] N. Li and S.-L. Zhu, Phys. Rev. D **86**, 074022 (2012).

[47] W. Meguro, Y.-R. Liu, and M. Oka, Phys. Lett. B **704**, 547 (2011).
[48] N. Li and S.-L. Zhu, Phys. Rev. D **86**, 014020 (2012).
[49] R. Machleidt, K. Holinde, and C. Elster, Phys. Rep. **149**, 1 (1987).
[50] R. Molina, T. Branz, and E. Oset, Phys. Rev. D **82**, 014010 (2010).